NASA TN D-64

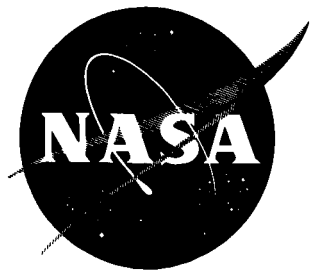

TECHNICAL NOTE

D-64

GRAPHICAL TRAJECTORY ANALYSIS

By Aaron S. Boksenbom

Lewis Research Center
Cleveland, Ohio

NATIONAL AERONAUTICS AND SPACE ADMINISTRATION

WASHINGTON

December 1959

TABLE OF CONTENTS

NATIONAL AERONAUTICS AND SPACE ADMINISTRATION

TECHNICAL NOTE D-64

GRAPHICAL TRAJECTORY ANALYSIS

By Aaron S. Boksenbom

SUMMARY

A simple graphical method for two-body trajectory problems is presented. The one basic graph used is composed simply of circles and straight lines. All features of trajectories appear on this map. Coasting trajectories correspond to circles on the graph. The transfer to new orbits on impulsive thrust, planar and nonplanar, is constructed on the same map. Approximations for continuous thrust and for cases of almost circular orbits are shown.

Examples are given for cases of transfer to new orbits, optimization on the velocity increment ΔV, interplanetary trips, and some rendezvous problems.

INTRODUCTION

There is a wide variety of problems in regard to the nature of orbits and trajectories of space flight ranging, say, from simple coasting paths to the optimization of thrust required for various missions. The need thus exists for a quick, simple, and practical method of estimating trajectory conditions and thrust required for many different types of cases.

The purpose of this report is to present a simple graphical method for trajectory analysis that can be applied to many types of trajectory problems. The one basic graph used is composed simply of circles and straight lines. Many trajectory variables of interest appear on this graph in this rather simple manner. Coasting trajectories correspond to circles on the graph. The transfer to a new trajectory on impulsive thrust is constructed on the same map, almost like realistic vector additions. Nonplanar thrust can be included.

The graphical method of reference 1 involves charts that must be prepared and does not include thrust. The method of reference 2 applies only for $e \to 0$ and is close to the methods of this report for that case; it does not include thrust.

Because many different variables appear in a simple fashion on the map presented herein, there are a number of ways of entering the map and many variables that can be read out simultaneously. This feature of the graphical method allows a large number of different types of problems to be analyzed with the same basic graphical construction. Examples in the use of this graphical method are given in the present report for cases of transfers to new orbits; optimum velocity increment ΔV; interplanetary, escape, and capture trajectories; and some rendezvous problems.

The simplicity of the graphical method suggests the possible use of its coordinate system in other types of trajectory analyses, such as in guidance problems or in general computer programing. The complete set of differential equations in this particular coordinate system is derived in the appendix.

SYMBOLS

A summary figure illustrating a general condition on any trajectory and the corresponding point in the X-Y map used for the graphical method is shown in figure 1(a) with the major symbols used in this report. To relate the position of the vehicle in space, the conventional three-dimensional geometry, shown in figure 1(b), is used.

e	eccentricity
F	thrust
G	gravitational constant
g	local acceleration due to gravity, $g = GM/r^2$
h	angular momentum, $h = rV_H = r^2\dot{\theta}$
i	inclination of plane of motion
K	identifies time lines (fig. 16)
M	mass of central body
m	mass of vehicle
R	radius on X-Y map, $R = hV/GM$
r	radial distance on trajectory
r_a	apogee distance

r_L semilatus rectum

r_p perigee distance

t time

t_p time of perigee crossing

V velocity

V_H velocity component in horizontal plane

V_R velocity component in radial direction

ΔV velocity increment due to thrust, $\overline{\Delta V} = \int \frac{\overline{F}}{m} dt$

X abscissa of map used in graphical method, $X = hV_H/GM = h^2/GMr = r_L/r$

x X-1

Y ordinate of map used in graphical method, $Y = hV_R/GM$

γ path angle

θ angle swept out by radius vector along trajectory

φ true anomaly, angle between direction of perigee and radius vector in plane of motion

ψ angle between planes of motion, before and after thrust (fig. 11)

Ω longitude of ascending node

ω angle between ascending node and direction of perigee in plane of motion

Unit vectors

$\hat{h}$ in direction of vector angular momentum

$\hat{n}$ in direction of ascending node

$\hat{r}$ in direction of radius vector

$\hat{V}$ in direction of velocity

$\hat{x},\hat{y},\hat{z}$ directions of fixed orthogonal coordinate system

$\hat{\theta}$ normal to $\hat{r}$, in plane of motion; $\hat{\theta} = \hat{h}\times\hat{r}$; triad $\hat{r}$, $\hat{\theta}$, $\hat{h}$ forms right-hand orthogonal system

Special symbols

$(\dot{})$ indicates time derivative, d/dt

$(\bar{})$ indicates vector

$(\hat{})$ indicates unit vector

$(\bar{})\cdot(\bar{})$ indicates scalar product

$(\bar{})\times(\bar{})$ indicates cross product

$(\ )^*$ used for specific conditions as noted in report

ANALYSIS

General Features of Graphical Method

The method consists of plotting trajectories on a graph with the abscissa X and ordinate Y given by

$$X = \frac{hV_H}{GM} = \frac{h^2}{GMr} = \frac{r_L}{r}$$

$$Y = \frac{hV_R}{GM}$$

where

V_H total velocity component in horizontal plane (normal to radial direction)

V_R velocity component in radial direction

h magnitude of angular momentum, $h = rV_H$

r_L magnitude of semilatus rectum, $r_L = h^2/GM$

This choice of coordinate system for the graph makes the method simple and easy to apply to a large variety of problems for the following reasons:

(1) For every point on any trajectory, there is a corresponding point on the graph. Along any actual trajectory, there is a corresponding curve traced out on the graph.

(2) For any coasting trajectory, the corresponding curve on the graph is a circle centered at the point $X = 1$, $Y = 0$ of radius equal to the eccentricity of the trajectory.

(3) Many other trajectory variables are directly and simply related to the X-Y coordinate system:

(a) Lines of constant e and φ form a polar coordinate system centered at the point $X = 1$, $Y = 0$.

(b) Lines of constant hV/GM and γ form another polar coordinate system centered at the point $X = 0$, $Y = 0$.

(c) The radial distance on the trajectory r is related to the abscissa, as $X = h^2/GMr$.

(d) Lines of constant $rV^2/GM = 2 + 2Er/GM$, where E is energy, are circles with center at $X = rV^2/2GM$, $Y = 0$, all of which go through the point $X = 0$, $Y = 0$.

(4) For noncoasting trajectories, there is a relatively simple construction on the graph for cases of both impulsive and continuous thrust.

In the appendix, the differential equations for the path in the X-Y plane are derived in order to show the general nature of the correspondence between any actual trajectory and its corresponding curve on the graph. For zero thrust, the differential equation is

$$(X - 1)dX + Y\,dY = 0$$

whose solution is

$$(X - 1)^2 + Y^2 = \text{Constant} = e^2$$

The expansion of the left side of this equation shows that the constant is the square of the eccentricity. The geometry in the X-Y plane for the eccentricity e is shown in figure 2. For easy reference, the point $X = 1$, $Y = 0$ is referred to herein as point Q, and the origin $X = 0$, $Y = 0$ as point 0.

It is well known that the true anomaly φ can be obtained from the following equation:

$$\frac{h^2}{GMr} = 1 + e \cos \varphi$$

which can be written $(X - 1)/e = \cos \varphi$. The true anomaly φ, corresponding to the X,Y point on the graph, is its angular rotation about point Q (fig. 2). Thus, the trajectory variables e and φ form a polar coordinate system centered at point Q on the graph, as shown in figure 3.

From the definition of X and Y it is obvious that

$$X^2 + Y^2 = (hV/GM)^2$$

and

$$Y/X = \tan \gamma.$$

Thus, the trajectory variables hV/GM and γ form another polar coordinate system centered at point 0 on the graph. In figure 4, the two polar coordinate systems are superposed on the graph. This map, and its construction, is the basis for the methods of this report.

Figure 5 is the same map with the detailed grid lines. All variables on the map are dimensionless. The unit distance should be chosen to give good accuracy for the particular problems at hand. It is believed that many trajectory problems can be solved with the aid of this map. Of course, a compass, straight-edge, scale, and protractor are sufficient without the aid of the grid guide lines.

Because of the many variables that appear on the map of figures 4 and 5, there are many different ways of entering the graph and many variables that can be read out simultaneously. This feature of the map means that a large number of different types of problems can be analyzed with the same map or construction. In a later section, it is shown that additional curves can be placed on the map to allow still more different ways of entering the graph and more variables that can be read out. One such family, mentioned previously, are lines of constant rV^2/GM, which are circles.

Coasting Trajectories

For zero thrust, the eccentricity is constant. Thus, all coasting trajectories correspond to circles on the graph. All circular coasting orbits correspond to point Q. Elliptic coasting orbits ($0 < e < 1$) correspond to the circles, centered at point Q, of radii from 0 to 1. The parabolic coasting orbit ($e = 1$) corresponds to the unit circle on the graph. Hyperbolic coasting orbits ($e > 1$) correspond to circles of radii greater than 1. These circles do not close; their intersection with the Y-axis gives the asymptotic conditions as $r \to \infty$.

As $d\varphi = d\theta$ for zero thrust (appendix) and the definition of θ requires that $d\theta/dt \geq 0$, motion on the graph corresponding to a coasting trajectory is always counterclockwise. Consider the coasting trajectory in figure 6 with, say, $e = 0.5$ corresponding to the path on the graph from points 1 to 2. The angle (1, Q, 2) is $\theta_2 - \theta_1$, the angle swept out by the radius vector along the trajectory. As the angular momentum h is also constant, the radial distance on the trajectory is inversely proportional to X, and $r_2/r_1 = X_1/X_2$. Also, it is apparent that the X axis to the right of point Q is the locus of perigees and to the left of point Q is the locus of apogees. The radial distance R on the map to the origin is hV/GM. Thus, the velocity on the trajectory is proportional to R, and $V_2/V_1 = R_2/R_1$. The path angles on the trajectory γ_1 and γ_2 appear directly on the graph of figure 6.

As another example, suppose a satellite is to be injected into orbit with an eccentricity $e = 0.25$. Then the possible burnout conditions correspond to the circle of $e = 0.25$ on the graph of figure 7. If the burnout path angle is also specified, say 10°, then burnout corresponds to the intersection on the map of the $e = 0.25$ circle and the $\gamma = 10^\circ$ line. Figure 7 shows a double-valued solution for this case, points 1 and 2. There is obviously a maximum path angle at burnout that could be specified. If a greater path angle were specified, there would be no intersection between the e-circle and the γ-line in figure 7. In this example and those in later sections, such impossible cases and other trajectory ambiguities and singularities are clearly defined by the use of the X-Y plane.

Impulsive Thrust

Planar thrust. - The same graph is easily adapted for impulsive thrusts. On the graph of figure 8, points 1 and 2 correspond to conditions on the trajectory before and after impulsive thrust, respectively. The vector between these two points is not $\overline{\Delta V}$, as the scale factor h/GM is not necessarily constant. The graphical construction is in two steps. A vectorlike addition of $h_1\overline{\Delta V}/GM$ to point 1 gives an intermediate point A; that is,

$$X_A = X_1 + \frac{h_1}{GM}(V_{2H} - V_{1H}) = \frac{h_1 V_{2H}}{GM} = \frac{h_1 h_2}{GMr}$$

$$Y_A = Y_1 + \frac{h_1}{GM}(V_{2R} - V_{1R}) = \frac{h_1 V_{2R}}{GM}$$

$$\frac{Y_A}{X_A} = \frac{V_{2R}}{V_{2H}} = \tan \gamma_2$$

The lines in the triangle (0, 1, A) are exactly like the vector addition of $\overline{\Delta V}$ to $\overline{V}_1$, with scale factor h_1/GM; the three vectors appear on the graph in realistic relation to each other and to the fixed $\hat{r},\hat{\theta}$ unit vectors, as shown on the sketch in figure 8.

Points A and 2 lie on the same γ_2 line. A simple relation between points 1, A, and 2 is obtained by noting that $X_A^2 = X_1X_2$. With this construction, point 2 can be found, given point 1 and $\overline{\Delta V}$; or $\overline{\Delta V}$ can be found, given points 1 and 2. Point 2 on the graph is then the start of a new coasting path along the circle (e = const.) on which it lies.

It is helpful to note the relations between going from points 1 to 2 and going from points 2 to 1. For the latter case, the first step is a vectorlike addition of $-(h_2\overline{\Delta V}/GM)$ to point 2, giving the intermediate point B; that is,

$$X_B = X_2 - \frac{h_2}{GM}(V_{2H} - V_{1H}) = \frac{h_2V_{1H}}{GM} = \frac{h_1h_2}{GMr} = X_A$$

$$Y_B = Y_2 - \frac{h_2}{GM}(V_{2R} - V_{1R}) = \frac{h_2V_{1R}}{GM}$$

$$\frac{Y_B}{X_B} = \frac{V_{1R}}{V_{1H}} = \tan \gamma_1$$

Points B and 1 lie on same γ_1 line. The relation between points 1, B, and 2 is the same as before, as

$$X_B = X_A$$

that is,

$$X_B^2 = X_1X_2$$

The construction for both forward and backward impulsive thrust is shown in figure 9. The fact that $X_A = X_B$ and lines 1A and 2B are parallel gives a further aid in the graphical construction. For example, starting at point 1 and adding $h_1\overline{\Delta V}/GM$ give point A and the γ_2 line. The intersection of the X_A vertical line and the γ_1 line gives point B. Drawing a line through point B, parallel to the line 1A, gives point 2 as its intersection with the γ_2 line. This construction would obviate the use of the formula $X_A^2 = X_1X_2$. The exception is the case of tangential thrust where $\gamma_1 = \gamma_2$ and the figure 1A2B lies on a line; in this case, the formula $X_A^2 = X_1X_2$ or $R_A^2 = R_1R_2$ can be used.

The values of the new orbital elements, after impulsive thrust, are self-evident. The eccentricity appears on the map. The angular momentum is given by

$$\frac{h_2}{h_1} = \frac{X_A}{X_1} = \frac{X_2}{X_A} = \left(\frac{X_2}{X_1}\right)^{1/2}$$

in figures 8 and 9. The rotation of the polar axis of the trajectory is given by

$$\omega_2 - \omega_1 = \varphi_1 - \varphi_2 = \text{Angle } (2, Q, 1)$$

in figures 8 and 9.

Direction reversal, planar thrust. - If, in the construction shown in figure 8, point A should lie to the left of the vertical axis, it means that the direction of motion has reversed. In this case, the mirror image of point A is used on the right of the vertical axis to complete the construction in figure 8. Subsequent coasting is still counterclockwise on the map, but the sense of the change in θ is reversed. Also, given points 1 and 2 on the map, there are two $\Delta\bar{V}$'s corresponding to the two mirror images for point A. These two $\Delta\bar{V}$'s would give the two types of trajectories sketched in figure 10.

Nonplanar thrust. - If $\Delta\bar{V}$ is not in the plane of motion, the construction in figure 8 still holds in terms of $(V_{2R} - V_{1R})$ and $(V_{2H} - V_{1H})$. While $(V_{2R} - V_{1R})$ is still the radial component of $\Delta\bar{V}$, the quantity $(V_{2H} - V_{1H})$ is not a component of $\Delta\bar{V}$. A separate construction is required to obtain this quantity. This construction is shown below the map of figure 11. This separate construction is essentially the velocity diagram in the horizontal plane. The unit vectors $\hat{\theta}_1$, $\hat{\theta}_2$, $\hat{h}_1$, and $\hat{h}_2$ are shown to identify directions. The vector line CD represents the total component of the impulse in the horizontal plane. The vector line OD represents V_{2H}, in direction $\hat{\theta}_2$. The length OD equals X_A and must be transferred to X-axis as shown in figure 11. The angle ψ is that between the two planes of motion, before and after thrust. On the map, the vector line 1E represents the total component of the impulse in the initial plane of motion.

Direction reversal, nonplanar thrust. - If, in the construction shown in figure 11, the point E should lie to the left of the vertical axis, it means - as in the case of planar thrust - that the direction of motion has reversed. In this case, the mirror image of point E is used on the right of the vertical axis to complete the construction in figure 11. Subsequent coasting is still counterclockwise on the map, but the sense of the change in θ is reversed.

Now, given points 1 and 2 on the map, X_A is uniquely determined by $X_A^2 = X_1 X_2$. On the construction below the map of figure 11, the length OD equals X_A. Thus, point D can lie anywhere on the circle of length X_A around point O. There are thus an infinite number of possible $\Delta\bar{V}$'s as the angle between the two planes ψ varies from 0° to 360°. For $90^\circ < \psi < 270^\circ$, point E lies to the left of the vertical axis corresponding to the direction reversal.

Continuous Thrust

One way of handling a continuous thrust by the graphical procedure just presented is to approximate the continuous thrust by a series pulse-coast-pulse-coast-etc. Figure 12 shows the construction of a pulse-coast and of a coast-pulse beginning at the same point 1. Path 1A23 is pulse 1A2 and then coast 23. Path 14B5 is coast 14 and then pulse 4B5.

It seems that the pulse-coast-etc. approximation should be made relative to the time integral of thrust-mass ratio. Figure 13 shows a component of $\int \frac{\bar{F}}{m}\,dt$. The approximate pulse-coast curve is the step function shown in figure 13. For this step function, horizontal parts are coasts, and vertical steps are the magnitudes of $\Delta\bar{V}$ pulses. The abscissa scale may be time or position.

In the appendix, the general exact differential equations for the path in the X-Y plane are derived. They are:

$$\frac{dX}{d\theta} = -Y + 2\left(\frac{\bar{F}}{mg} \cdot \hat{\theta}\right)$$

$$\frac{dY}{d\theta} = (X - 1) + \frac{Y}{X}\left(\frac{\bar{F}}{mg} \cdot \hat{\theta}\right) + \left(\frac{\bar{F}}{mg} \cdot \hat{r}\right)$$

$$\frac{dg}{g\,d\theta} = -2\,\frac{Y}{X}$$

where g is the local acceleration due to gravity, $g = GM/r^2$. These equations are valid for general three-dimensional motion. Note that the component of thrust normal to the instantaneous plane of motion does not appear; this component merely rotates the plane of motion. In these equations, the independent variable is θ, the angle swept out by the radius vector along the trajectory. Elapsed time, if required, is obtained from

$$\frac{dt}{d\theta} = \frac{(GM)^{1/4}}{g^{3/4}\,X^{1/2}}.$$

Thus, a gross approximation is obtained as shown in figures 12 and 13, and an exact form is given by the preceding differential equations. Further analysis for continuous thrust is beyond the scope of this report.

Almost Circular Orbits, $e \rightarrow 0$

It was noted previously that all variables on the map of figures 4 and 5 are dimensionless and that the unit distance should be chosen to give good accuracy for the particular problem at hand. For the case of $e \rightarrow 0$, an expansion of the map in the region of the point Q is needed. In this region the circles centered at point 0 are almost vertical lines, and the rays from point 0 are almost horizontal lines. Thus, a single set of polar coordinates suffices; the horizontal scale gives both r and V, and the vertical scale gives γ.

The approximate map for cases where $e \rightarrow 0$ is shown in figure 14. It is convenient to introduce the variables r^* and V^*, which essentially replace the scale factor h/GM. These variables are the radial distance and approximate velocity when $\varphi = 90^\circ$, a kind of average conditions.

The construction for impulsive thrust is shown in figure 15. The vector from point 1 to point A is $\Delta\bar{V}/V_1^*$. Point 2 lies to the right of point A such that $x_1 + x_2 = 2x_A$. Point 2 on the map is then the start of a new coasting path along the circle (e = const.) on which it lies.

The new scale factors are given by

$$x_2 - x_1 = \frac{r_2^* - r_1^*}{r} = 2\,\frac{V_1^* - V_2^*}{V_1^*}$$

The angle (2,Q,1) in figure 15 is $\omega_2 - \omega_1$, the rotation of the polar axis of the orbit. The value of velocity after thrust is obtained from $2\left[(V_2 - V_1)/V_1^*\right] = x_2 - x_1$. The value of path angle after thrust is read directly from figure 15.

Vertical Flight, $h = 0$

This is the one case where the graphical method breaks down. The scale factor on both axes of figure 5 is h/GM, and, when $h = 0$, the map degenerates into the point 0. Of course, the case $h = 0$, which is vertical flight, is relatively simple for straightforward calculations.

APPLICATIONS

Additional Curves For Map

Equations for various families of curves. - For certain problems it may be convenient to have certain families of curves on the map of figures 4 and 5. A list of equations for some of these follows:

(1): $\frac{G^2M^2}{h^3}(t - t_p) = \text{Const.}; \int_0^{\varphi} \frac{dy}{(1 + e \cos y)^2} = \frac{G^2M^2}{h^3}(t - t_p)$

(2): $\frac{r_p}{r} = \text{Const.}; \frac{X}{1 + e} = \frac{r_p}{r}$

(3): $\frac{r_a}{r} = \text{Const.}; \frac{X}{1 - e} = \frac{r_a}{r}$

(4): $\frac{rV^2}{GM} = \text{Const.}$; circles with center at $\left(\frac{rV^2}{2GM}, 0\right)$, radius $= \frac{rV^2}{2GM}$, all of which go through point (0,0).

Note that $rV^2/GM = 2 + 2Er/GM = 2 - r/a$, where E is energy, $V^2/2 - GM/r$, and a is magnitude of semimajor axis.

(5): $\frac{b_1}{r} = \text{Const.}; \frac{X}{(rV^2/GM) - 2} = \left(\frac{b_1}{r}\right)^2$

where b_1 is impact parameter of hyperbolic orbits, $h = b_1V(r \to \infty)$.

For the general condition $r = r^*$, $\varphi = \varphi^*$, $\gamma = \gamma^*$, and so forth,

(6): $\frac{r^*}{r}, \gamma^*$ of interest, as on reentry; $X^2\left(\frac{r}{r^*}\right)^2 \sec^2 \gamma^* - 2X \frac{r}{r^*} + 1 = e^2$

(7): $\frac{r^*}{r}, \varphi^*$ of interest; $\frac{r^*}{r} = \frac{1 + e \cos \varphi}{1 + e \cos \varphi^*}$

The only variable that really does not appear on the map of figure 5 is time. Thus, only the first of the preceding families of curves is necessary. The others may be convenient but, as shown in later examples, are not strictly necessary.

Time lines. - As just shown, lines of $(G^2M^2/h^3)(t - t_p) = K$ can be placed on the map of figure 5. Such a family of curves is shown in figure 16. On this figure, lines of constant K are drawn symmetrically

with respect to the X-axis. Thus, above the X-axis, going from perigee to apogee, $K = (G^2M^2/h^3)(t - t_p)$, which gives time elapsed since the last perigee crossing. Below the X-axis, approaching the perigee, $K = (G^2M^2/h^3)(t_p - t)$, which gives time to go to the next perigee crossing. Along the X-axis, to the right of point Q, $K = 0$. Along the X-axis from the points 0 to Q, $K = \pi(1 - e^2)^{-3/2}$, which indicates the half-period.

By using these curves, the time elapsed during any coasting phase is easily obtained. Figure 17 indicates four conditions along a coasting path. Considering the definition of the K-lines of figure 16 gives the following four cases:

(1): $$\frac{G^2M^2}{h^3}(t_2 - t_1) = K_2 - K_1$$

(2): $$\frac{G^2M^2}{h^3}(t_4 - t_3) = K_3 - K_4$$

(3): $$\frac{G^2M^2}{h^3}(t_1 - t_4) = K_1 + K_4$$

(4): $$\frac{G^2M^2}{h^3}(t_3 - t_2) = 2K_A - K_2 - K_3$$

Note that $K_A = \frac{G^2M^2T}{h^3 2} = \pi(1 - e^2)^{-3/2}$ where T is period of orbit.

By using these curves, the change in t_p on impulsive burning is easily obtained. For example, if points 1 and 2 are points on the map before and after impulsive thrust, then

$$\frac{G^2M^2}{h_1^3}(t - t_{p,1}) = K_1$$

$$\frac{G^2M^2}{h_2^3}(t - t_{p,2}) = K_2$$

where both points 1 and 2 are considered to be above the X-axis. It follows that

$$\frac{G^2M^2}{h_1^3}(t_{p,1} - t_{p,2}) = \frac{h_2^3}{h_1^3}K_2 - K_1$$

$$= \left(\frac{X_2}{X_1}\right)^{3/2} K_2 - K_1$$

or

$$\frac{t_{p,1} - t_{p,2}}{t - t_{p,1}} = \left(\frac{X_2}{X_1}\right)^{3/2} \frac{K_2}{K_1} - 1$$

Transfer To New Orbit

Suppose it is desired to burn at a definite position along orbit 1, say point 1a in figure 18, to transfer to a new orbit with parameters e_2, h_2. Then X_2 is determined by $X_{2a}/X_{1a} = h_2^2/h_1^2$; the intersection of this X_2 line with the e_2 circle determines point 2a. Point Aa and the corresponding $\Delta\bar{V}$ follow as in figure 8.

The angle (2a, Q, 1a) gives $\omega_2 - \omega_1$. For point 1 at various positions along the e_1 circle, this rotation of the polar axis will vary. If, for example, no rotation of the polar axis is desired, then points Q, 2, and 1 must lie on a straight line. Such a line may be line Q-2b-1b, which is such that $X_{2b}/X_{1b} = h_2^2/h_1^2$. Point Ab and the required $\Delta\bar{V}$ to transfer to orbit with parameters e_2, h_2, $\omega_2 = \omega_1$ follow as in figure 8. The correct position along orbit 1 at which to burn so as to keep $\omega_2 = \omega_1$ is also obtained.

Optimum ΔV

Case 1. - Suppose it is desired to burn along orbit 1 at a fixed position (point 1 of fig. 19) so that the subsequent trajectory has a fixed perigee. The freedom in the specification of this problem allows an optimization on $\Delta\bar{V}$.

The perigee point of the new orbit lies along the X-axis to the right of point Q in figure 19. For each such possible perigee point p, the circle of constant e can be traced backwards to its point 2, which is determined by $X_p/X_2 = r_1/r_{p,2}$. The possible points 2 so generated actually form a curve; this curve is the line of r/r_p = constant, which was mentioned in a previous section. The corresponding points A are generated as before (fig. 8); they also form a curve. The minimum ΔV is the shortest distance from point 1 to the curve of points A. The optimum path is shown as the solid line in figure 19.

The minimum ΔV in magnitude and direction is so obtained. In addition to obtaining the optimum ΔV, all other possible ways of achieving the fixed perigee are shown in figure 19.

Case 2. - Suppose it is desired to burn along orbit 1 at a fixed position (point 1 of fig. 20) so that the new orbit will pass through $r = r^*$, $\gamma = \gamma^*$. This is the requirement that a reentry may give. The new orbit will reach $\gamma = \gamma^*$ along the line of $\gamma = \gamma^*$ on the map. For each such possible final point E, the circle of constant e can be traced backwards to its point 2, which is determined by $X_E/X_2 = r_1/r^*$. The corresponding points A are generated as before. The minimum ΔV can then be seen by inspection; the optimum path is shown in figure 20 as a solid line. This case actually includes case 1 if $\gamma^* = 0$.

Case 3. - Suppose it is desired to simply change the orbital parameters to e_2, h_2, and the position of burning along orbit 1 can be chosen so as to minimize ΔV. Point 1 lies along the circle of e_1 (fig. 21). For each such possible point, X_2 is determined by $X_2/X_1 = h_2^2/h_1^2$. The intersection of this X_2-line and the e_2 circle determines the corresponding point 2, as shown in figure 21. The points A and $\Delta\bar{V}$'s are found as before. The minimum ΔV is seen by inspection.

Additional cases. - There are many possible optimization problems that can be posed. For example, among the variables ω,h,e; r,φ; V,γ,V_H,V_R; t there are of the order of $\frac{10!}{8!2!} = 45$ cases. Even this does not exhaust the possible cases as various functions of these variables may be considered. It is believed that most of these cases can be solved graphically by using the map presented in this report. The variable time requires the curves of constant $t - t_p$ as discussed before.

Interplanetary Trajectories

The usual two-body trajectories are used such that inside the sphere of influence of a planet the sun's field is neglected and outside this region the planet's field is neglected. On the boundary of this region,

$$\bar{V}_{C,A} = \bar{V}_A + \bar{V}_{h,A}$$

where

$\bar{V}_{C,A}$ velocity of vehicle relative to sun on sphere of influence of planet A

$\bar{V}_A$ velocity of planet A relative to sun

$\bar{V}_{h,A}$ velocity of vehicle relative to planet A on sphere of influence of planet A

The hyperbolic velocity $\overline{V}_{h,A}$ acts like a $\Delta\overline{V}$ thrust impulse added to the velocity of the planet.

As an example, take the minimum-energy transfer orbits between planets A and B, which are in circular orbits around the sun. Figure 22 is the map of figure 5 for this example. Starting at point 1, which represents the orbit of planet A, $\overline{V}_{h,A}$ is added to the planet as if it were a $\Delta\overline{V}$. This increment is added tangentially, as shown. The coasting path around the sun is path 23, where $X_2/X_3 = r_B/r_A$. The hyperbolic velocity at planet B is negative as shown, corresponding to the vehicle moving more slowly than planet B. The return trip is similar, going from points 1 to 3 and coasting from 3 to 2 along the same semicircle but below the X-axis, and so forth.

The hyperbolic velocities $\overline{V}_{h,A}$ and $\overline{V}_{h,B}$ determine the required $\Delta\overline{V}$'s in the neighborhood of planets A and B. For example, take the case of starting in a circular satellite orbit and adding, tangentially, a $\Delta\overline{V}$ to reach $\overline{V}_{h,A}$. Figure 23 is the graphical construction for this case. Points 1 and 2 are points on the map before and after thrust. Path 23 is the coasting path. The intersection of this circle with the vertical axis (point 3) gives hyperbolic conditions. For this problem it is most convenient to use the circles of constant rV^2/GM as noted before (section "Additional Curves for Map"); or, for $\gamma_2 = 0$, $X_2 = rV_2^2/GM = 2 + (rV_{h,A}^2/GM)$. This would determine X_2 and thus the $\Delta\overline{V}$ required. The angle shown, β, determines the angular direction with which the vehicle leaves planet A.

Some Rendezvous Problems

Orbit geometry in a plane. - The intersection of two orbits is defined by

(1): $$\omega_1 + \varphi_1 = \omega_2 + \varphi_2$$

(2): $$r_1 = r_2$$

If, on the map of figure 24, points 1a and 2a are the conditions on orbits 1 and 2 at their intersection, then the preceding two conditions become

(1): $$\text{Angle } (2a, Q, 1a) = \omega_2 - \omega_1$$

(2): $$\frac{X_{2a}}{X_{1a}} = \frac{h_2^2}{h_1^2}$$

The tangency of two orbits requires a third condition:

(3): $$\gamma_1 = \gamma_2$$

If, in figure 24, points 1b and 2b are the conditions on orbits 1 and 2 at their tangency, then

(1): $$\text{Angle } (2b, Q, 1b) = \omega_2 - \omega_1$$

(2): $$\frac{X_{2b}}{X_{1b}} = \frac{h_2^2}{h_1^2}$$

(3): Points 0, 1b, and 2b lie on straight line

For the intersection or tangency condition, it would be convenient to have a drawing instrument (or two-arm protractor) centered at the point Q with two arms having the fixed included angle $\omega_2 - \omega_1$. Rotation of both arms until $X_2/X_1 = h_2^2/h_1^2$ gives conditions at the intersection of two orbits. If, at this condition, points 0, 1, and 2 lie on a straight line, then the two orbits are also tangent at this point.

Transfer orbit tangent to initial and final orbits. - Consider a rendezvous maneuver involving two tangential ΔV's. Initial orbit is e_1, h_1, ω_1; transfer orbit is e_2, h_2, ω_2; final orbit is e_3, h_3, ω_3. The conditions of tangency (fig. 25) require:

(1): $$\text{Angle } (2a, Q, 1) = \omega_2 - \omega_1$$

(2): $$\frac{X_{2a}}{X_1} = \frac{h_2^2}{h_1^2}$$

(3): Points 0, 1, and 2a on straight line

(4): $$\text{Angle } (3, Q, 2b) = \omega_3 - \omega_2$$

(5): $$\frac{X_3}{X_{2b}} = \frac{h_3^2}{h_2^2}$$

(6): Points 0, 2b, and 3 on straight line

As h_2 and ω_2 are not of interest here, these six conditions reduce to the following four conditions:

(1): Angle (2a, Q, 1) + angle (3, Q, 2b) = $\omega_3 - \omega_1$

(2): $$\frac{X_{2a}X_3}{X_1X_{2b}} = \frac{h_3^2}{h_1^2}$$

(3): Points 0, 1, and 2a on straight line

(4): Points 0, 2b, and 3 on straight line

Starting with point 1, a point 2a, which satisfies condition (3), can be tried. This gives angle (3, Q, 2b) by condition (1), and also X_3/X_{2b} by condition (2). Using the two-arm protractor with included angle fixed at angle (3, Q, 2b), rotate it until points 0, 2b, and 3 lie on a straight line (condition (4)). Then check to see if X_3/X_{2b} is correct. If not, try a different point 2a, and so forth. When, by such trial and error, points 2a, 2b, and 3 are determined, the ΔV's are readily found as shown in figure 25.

Transfer orbit of minimum ΔV. - The transfer orbit of the previous section considered only tangential ΔV's. Suppose the problem is to transfer from an initial orbit of e_1, h_1, ω_1 to a final orbit of e_3, h_3, and ω_3 using two ΔV's such that the total ΔV is a minimum. Referring to figure 26, there are two conditions:

(1): Angle (2a, Q, 1) + angle (3, Q, 2b) = $\omega_3 - \omega_1$

(2): $$\frac{X_{2a}X_3}{X_1X_{2b}} = \frac{h_3^2}{h_1^2}$$

The solution for minimum ΔV is a trial and error optimization for points 1 and 2a. Starting with any point 1 and any point 2a, angle (3, Q, 2b) is determined by condition (1), and X_3/X_{2b} is determined by condition (2). With the included angle fixed at angle (3, Q, 2b), the two-arm protractor is rotated until points 2b and 3 satisfy proper X_3/X_{2b}, condition (2). The total ΔV is obtained as in figure 26 and noted. Various points 2a are tried until minimum ΔV is obtained. Then, starting over with various points 1, optimize with respect to various points 1.

CONCLUDING REMARKS

A simple, quick, and practical graphical method for trajectory analysis, applicable to many different types of problems, has been described herein. A summary figure showing the correspondence between trajectory conditions and the X-Y map used for the graphical construction is shown in figure 1(a). The upper part of the summary figure shows point (1) as the instantaneous condition; the orbit shown would be that for subsequent coasting. The lower part of the figure shows the corresponding point 1 in the X-Y plane. Many trajectory variables appear rather simply in this plane. The variables e, φ are the polar coordinates around the point Q. The variables hV/GM, γ are polar coordinates around the point O. The radial distance on the trajectory r is related to X. The subsequent coasting orbit, starting at point 1, is the circle on the map of constant e that goes through the point 1 as shown in figure 1(a). The true anomaly φ appears directly on the map in a realistic manner as shown in figure 1(a). The only variable that does not appear directly on the map or cannot easily be inferred from it is time. Figure 16 shows the set of time lines superposed on the map.

The transfer to a new orbit on impulsive thrust was constructed on the same map, almost like realistic vector addition of velocities, both for planar and nonplanar cases. For continuous thrust, the exact differential equations describing the corresponding path of the operating point in the X-Y plane were derived. Approximations for continuous thrust in terms of a series pulse-coast-pulse-coast-etc. were shown. Another approximation for the case of almost circular orbits ($e \to 0$), which simplified the graphical construction even further, was described.

Because of the many variables that appear on the X-Y map, there are many different ways of entering the map and many variables that can be read out simultaneously. This feature allows a large number of different types of problems to be analyzed with the same construction. Examples given in the report range from simple coasting paths to optimization of ΔV for various cases and to several types of rendezvous problems.

Lewis Research Center
National Aeronautics and Space Administration
Cleveland, Ohio, August 11, 1959

APPENDIX - DERIVATION OF EQUATIONS OF MOTION IN COORDINATES OF GRAPHICAL METHOD

Basic Kinematics

For any unit vector, say $\hat{e}$, of constant length, $\hat{e} \cdot \hat{e} = 1$. On taking the time derivative of this equation, $\hat{e} \cdot \dot{\hat{e}} = 0$. Thus, for any unit vector, $\hat{e}$ and $\dot{\hat{e}}$ are normal.

Let the plane of the paper of figure 27 be the instantaneous $\bar{r},\bar{V}$ plane of motion. The vector angular momentum is defined by $\bar{h} = \bar{r} \times \bar{V}$. Thus, $\hat{h}$ is normal to the $\bar{r}$ - $\bar{V}$ plane. A $\hat{\theta}$ direction is defined as $\hat{\theta} = \hat{h} \times \hat{r}$. Thus $\hat{\theta}$ lies in the $\bar{r}$ - $\bar{V}$ plane, normal to $\hat{r}$, such that the triad $\hat{r}$, $\hat{\theta}$, $\hat{h}$ forms an orthogonal right-hand system.

The magnitude of the angular momentum is obtained from the preceding definition of $\bar{h}$ as follows:

$$h = \hat{h} \cdot \bar{h} = \hat{h} \cdot (\bar{r} \times \bar{V}) = r(\bar{V} \cdot \hat{\theta})$$

The components of the velocity are obtained from the definition

$$\bar{V} = \dot{\bar{r}} = \hat{r}\dot{r} + r\dot{\hat{r}}$$

The vector $\dot{\hat{r}}$ thus lies in the $\bar{r}$ - $\bar{V}$ plane; as it is also normal to $\hat{r}$, it must lie in the $\hat{\theta}$ direction. Thus, $\dot{\hat{r}} = \dot{\theta}\hat{\theta}$, which also serves as the definition for $d\theta$ (or θ), as shown in figure 27. The expression for velocity becomes

$$\left.\begin{aligned} \bar{V} &= \dot{r}\hat{r} + (r\dot{\theta})\hat{\theta} \\ \bar{V} \cdot \hat{r} &= V_R = \dot{r} \\ \bar{V} \cdot \hat{\theta} &= V_H = r\dot{\theta} \end{aligned}\right\} \qquad \text{(A1)}$$

The magnitude of angular momentum is

$$h = r(\bar{V} \cdot \hat{\theta}) = r^2\dot{\theta} \qquad \text{(A2)}$$

The angle θ is that angle swept out by the radius vector along the trajectory. For general nonplanar motion, θ would be the accumulated angle on the curved surface generated by the radius vector. From equation (A2), it is evident that $d\theta/dt \gtrless 0$, so that $d\theta$ (or θ) can be used as the independent variable of the motion, replacing the usual independent variable dt (or t). The exception is the case of radial motion on the trajectory, where $d\theta/dt = 0$.

To get the time derivatives of h, $\hat{h}$, and $\hat{\theta}$, $\dot{\bar{h}} = \frac{d}{dt}(\bar{r} \times \bar{V}) = \bar{r} \times \dot{\bar{V}}$, or $\dot{h}\hat{h} + h\dot{\hat{h}} = \bar{r} \times \dot{\bar{V}}$. On taking the scalar product of this equation with $\hat{h}$, $\hat{\theta}$, and $\hat{r}$ in turn,

$$\dot{h} = \hat{h} \cdot (\bar{r} \times \dot{\bar{V}}) = r(\dot{\bar{V}} \cdot \hat{\theta}) \tag{A3}$$

$$h(\dot{\hat{h}} \cdot \hat{\theta}) = \hat{\theta} \cdot (\bar{r} \times \dot{\bar{V}}) = -r(\dot{\bar{V}} \cdot \hat{h})$$

$$h(\dot{\hat{h}} \cdot \hat{r}) = \hat{r} \cdot (\bar{r} \times \dot{\bar{V}}) = 0$$

and, thus,

$$h\dot{\hat{h}} = -r(\dot{\bar{V}} \cdot \hat{h})\hat{\theta} \tag{A4}$$

From $\hat{\theta} = \hat{h} \times \hat{r}$,

$$\dot{\hat{\theta}} = -\dot{\theta}\hat{r} + \frac{r}{h}(\dot{\bar{V}} \cdot \hat{h})\hat{h} \tag{A5}$$

The components of the acceleration are obtained from the time derivative of the first of equations (A1).

$$\dot{\bar{V}} = (\ddot{r} - r\dot{\theta}^2)\hat{r} + (r\ddot{\theta} + 2\dot{r}\dot{\theta})\hat{\theta} + (\dot{\bar{V}} \cdot \hat{h})\hat{h} \tag{A6}$$

where it is noted that the magnitude of the $\hat{\theta}$ component is $\dot{h}/r$.

Kinematics in X-Y Plane

The X and Y coordinates of the graph used in the methods of this report can be defined as follows:

$$X = \frac{hV_H}{GM} = \frac{hr\dot{\theta}}{GM} = \frac{h^2}{GMr}$$

$$Y = \frac{hV_R}{GM} = \frac{h\dot{r}}{GM}$$

Differentiation of these equations, using equations (A2), (A3), and (A6), gives

$$\frac{dX}{d\theta} = -Y + 2\left(\frac{\dot{\bar{V}}}{g} \cdot \hat{\theta}\right) \tag{A7}$$

$$\frac{dY}{d\theta} = X + \frac{Y}{X}\left(\frac{\dot{\bar{V}}}{g} \cdot \hat{\theta}\right) + \left(\frac{\dot{\bar{V}}}{g} \cdot \hat{r}\right) \tag{A8}$$

where

$$g = \frac{GM}{r^2}$$

and

$$\frac{dg}{g\, d\theta} = -2\,\frac{Y}{X} \tag{A9}$$

The preceding three equations give the path in the X-Y plane with θ as the independent variable or parameter. Elapsed time dt (or t) is given by

$$\frac{dt}{d\theta} = \frac{(GM)^{1/4}}{g^{3/4}\, X^{1/2}} \tag{A10}$$

Three-Dimensional Kinematics

To relate the position of the vehicle in space, consider the conventional geometry (ref. 3) as shown in figure 1(b), where $\hat{x}$, $\hat{y}$, $\hat{z}$ are fixed directions. The angle between $\hat{z}$ and $\hat{h}$ is the inclination i. The unit vector direction $\hat{n}$ is along the intersection of the $\hat{x}$, $\hat{y}$ plane and the $\hat{r}$, $\hat{v}$ plane, that is, the direction of the ascending node. Analytically,

$$\hat{z} \cdot \hat{h} = \cos i$$

$$\hat{z} \times \hat{h} = \hat{n} \sin i,\ 0 < i < 180^\circ$$

The angles Ω and $\omega + \varphi$ are defined by

$$\hat{x} \cdot \hat{n} = \cos \Omega,\ 0 < \Omega < 360^\circ$$

$$\hat{n} \cdot \hat{r} = \cos(\omega + \varphi),\ 0 < \omega + \varphi < 360^\circ$$

On taking the time derivatives of these four equations, first note that

$$h \sin i\, \frac{d\hat{n}}{dt} = (\hat{z} \times \hat{n}) r \sin(\omega + \varphi)(\dot{\bar{V}} \cdot \hat{h})$$

Then, the rates of change of ω, Ω, and i are

$$\left.\begin{aligned} h \sin i\, \frac{d}{dt}(\omega + \varphi - \theta) &= -r \sin(\omega + \varphi)\cos i(\dot{\bar{V}} \cdot \hat{h}) \\ h \sin i\, \frac{d}{dt}\Omega &= r \sin(\omega + \varphi)(\dot{\bar{V}} \cdot \hat{h}) \\ h\, \frac{di}{dt} &= r \cos(\omega + \varphi)(\dot{\bar{V}} \cdot \hat{h}) \end{aligned}\right\}$$

On using $d\theta$ as the independent variable, the preceding three equations become

$$X \frac{d}{d\theta} (\omega + \varphi - \theta) = -\sin(\omega + \varphi)\cot i \left(\frac{\dot{\bar{V}} \cdot \hat{h}}{g}\right) \tag{A11}$$

$$X \frac{d}{d\theta} \Omega = \frac{\sin(\omega + \varphi)}{\sin i} \left(\frac{\dot{\bar{V}} \cdot \hat{h}}{g}\right) \tag{A12}$$

$$X \frac{di}{d\theta} = \cos(\omega + \varphi)\left(\frac{\dot{\bar{V}} \cdot \hat{h}}{g}\right) \tag{A13}$$

Complete Set of Differential Equations of Motion

General case. - Equations (A7) to (A13) are a complete set of differential equations for the motion in terms of the variables X, Y, g, t, $\omega + \varphi$, Ω, and i as functions of θ with $\dot{\bar{V}} \cdot \hat{r}$, $\dot{\bar{V}} \cdot \hat{\theta}$, and $\dot{\bar{V}} \cdot \hat{h}$ as the inputs. There are seven equations, rather than the usual six, because the independent variable θ is, in general, merely a parameter of the motion.

From the definition of X and Y,

$$(X - 1)^2 + Y^2 = 1 + \frac{2h^2}{G^2M^2}\left(\frac{V^2}{2} - \frac{GM}{r}\right) = e^2$$

which is the usual definition of the eccentricity e. Also,

$$X = \frac{h^2}{GMr} = 1 + e \cos \varphi$$

by the usual definition of the true anomaly φ. It may be convenient to have the differential equations for e and φ. These are:

$$e \frac{de}{d\theta} = Y\left[\left(\frac{\dot{\bar{V}} \cdot \hat{r}}{g}\right) + 1\right] + \left[\frac{Y^2}{X} + 2(X - 1)\right]\left(\frac{\dot{\bar{V}} \cdot \hat{\theta}}{g}\right) \tag{A14}$$

$$e^2 \frac{d}{d\theta} (\varphi - \theta) = (X - 1)\left[\left(\frac{\dot{\bar{V}} \cdot \hat{r}}{g}\right) + 1\right] - Y \left(1 + \frac{1}{X}\right)\left(\frac{\dot{\bar{V}} \cdot \hat{\theta}}{g}\right) \tag{A15}$$

Inverse-square central gravitational field. - All the equations in this appendix up to this point are quite general; expressions for the acceleration $\dot{\bar{V}}$ and the gravitational field have not yet been specified. For the case of an inverse-square central gravitational field, the acceleration is

$$\dot{\bar{V}} = \bar{F}/m - g\hat{r}$$

where $\overline{F}$ is vector thrust and m is mass of vehicle. Then

$$\left.\begin{aligned} \frac{\dot{\overline{V}} \cdot \hat{r}}{g} &= \frac{\overline{F} \cdot \hat{r}}{mg} - 1 \\ \frac{\dot{\overline{V}} \cdot \hat{\theta}}{g} &= \frac{\overline{F} \cdot \hat{\theta}}{mg} \\ \frac{\dot{\overline{V}} \cdot \hat{h}}{g} &= \frac{\overline{F} \cdot \hat{h}}{mg} \end{aligned}\right\}$$

The seven differential equations of motion (eqs. (A7) to (A13)) then become

$$\left.\begin{aligned} \frac{dX}{d\theta} &= -Y + 2\left(\frac{\overline{F} \cdot \hat{\theta}}{mg}\right) \\ \frac{dY}{d\theta} &= (X - 1) + \frac{Y}{X}\left(\frac{\overline{F} \cdot \hat{\theta}}{mg}\right) + \left(\frac{\overline{F} \cdot \hat{r}}{mg}\right) \\ \frac{dg}{g\, d\theta} &= -2\,\frac{Y}{X} \\ \frac{dt}{d\theta} &= \frac{(GM)^{1/4}}{g^{3/4}\, X^{1/2}} \\ X\,\frac{d}{d\theta}(\omega + \varphi - \theta) &= -\sin(\omega + \varphi)\cot i\left(\frac{\overline{F} \cdot \hat{h}}{mg}\right) \\ X\,\frac{d}{d\theta}\,\Omega &= \frac{\sin(\omega + \varphi)}{\sin i}\left(\frac{\overline{F} \cdot \hat{h}}{mg}\right) \\ X\,\frac{di}{d\theta} &= \cos(\omega + \varphi)\left(\frac{\overline{F} \cdot \hat{h}}{mg}\right) \end{aligned}\right\} \qquad \text{(A16)}$$

For convenience, the differential equations for e and $\varphi - \theta$ can be written as follows:

$$\left.\begin{aligned} e\,\frac{de}{d\theta} &= Y\left(\frac{\overline{F} \cdot \hat{r}}{mg}\right) + \left[\frac{Y^2}{X} + 2(X - 1)\right]\left(\frac{\overline{F} \cdot \hat{\theta}}{mg}\right) \\ e^2\,\frac{d}{d\theta}(\varphi - \theta) &= (X - 1)\left(\frac{\overline{F} \cdot \hat{r}}{mg}\right) - Y\left(1 + \frac{1}{X}\right)\left(\frac{\overline{F} \cdot \hat{\theta}}{mg}\right) \end{aligned}\right\} \qquad \text{(A17)}$$

For a coasting path, $\hat{n}$ and ω are constant, and $\Delta\varphi = \Delta\theta$ = angle swept out by radius vector in the plane of motion (fig. 1(b)). For the case of impulsive thrust in the plane of motion, $\hat{n}$ is constant and $\Delta(\omega + \varphi) = 0$; thus, $\Delta\omega = -\Delta\varphi$.

REFERENCES

1. Sohn, Robert L.: A Proposed Kepler Diagram. ARS Jour., vol. 29, no. 1, Jan. 1959, pp. 51-54.

2. Luetjen, H. H., and Ramey, M. L.: Orbit Relationships. Space/Aero., vol. 31, no. 3, Mar. 1959, pp. 122; 126; 129; 134; 138.

3. Moulton, Forest Ray: An Introduction to Celestial Mechanics. Second revised ed., The Macmillan Co., 1947.

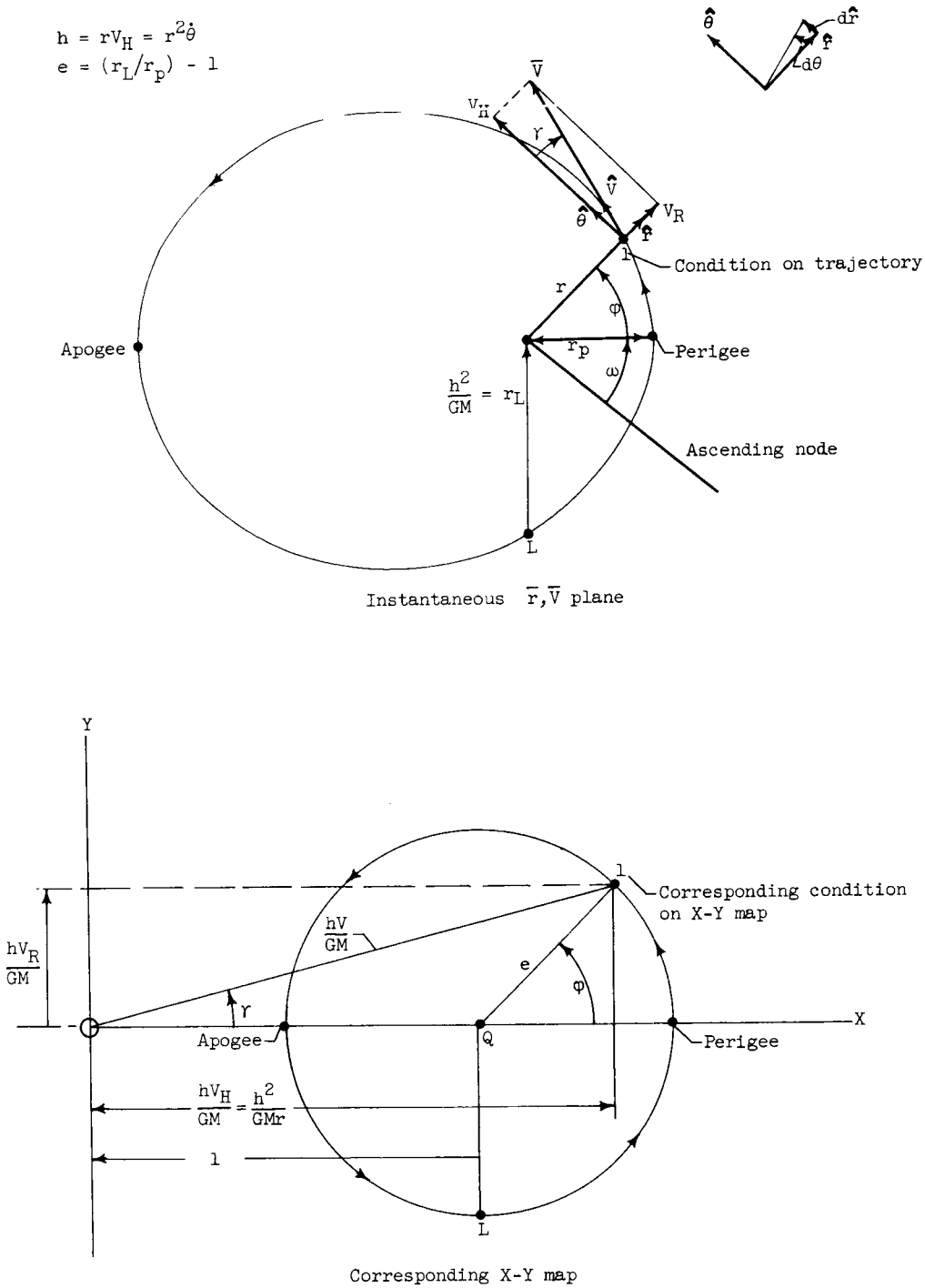

(a) Summary figure illustrating correspondence between trajectory conditions and points in coordinate system of graphical method.

Figure 1. - Mapping of trajectory conditions into X-Y plane and the space orientation, showing major symbols used in report.

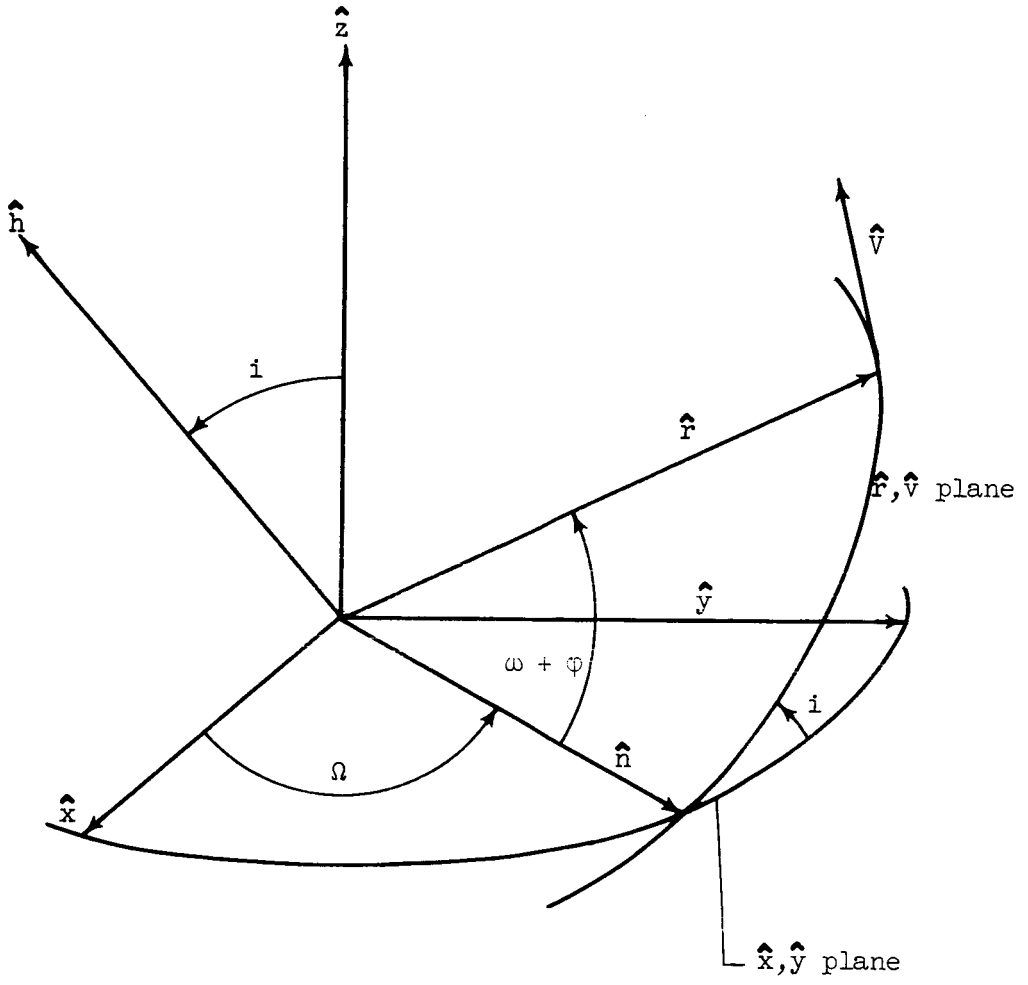

$\hat{z} \cdot \hat{h} = \cos i$

$\hat{z} \times \hat{h} = \hat{n} \sin i$

$\hat{x} \cdot \hat{n} = \cos \Omega$

$\hat{n} \cdot \hat{r} = \cos(\omega + \varphi)$

(b) Coordinate system used for space orientation.

Figure 1. - Concluded. Mapping of trajectory conditions into X-Y plane and the space orientation, showing major symbols used in report.

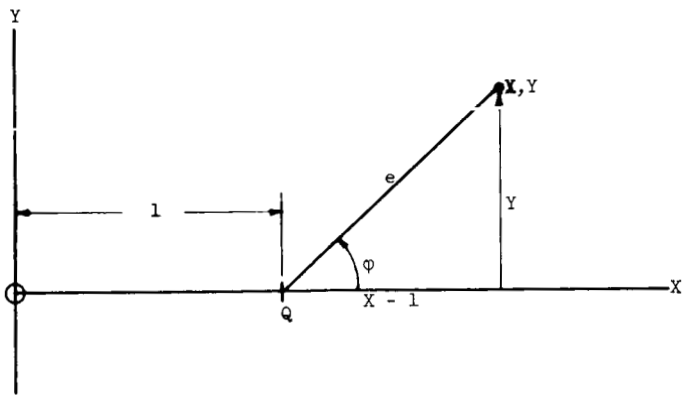

Figure 2. - Geometry in X-Y plane of graphical method for eccentricity, e, and true anomaly, φ.

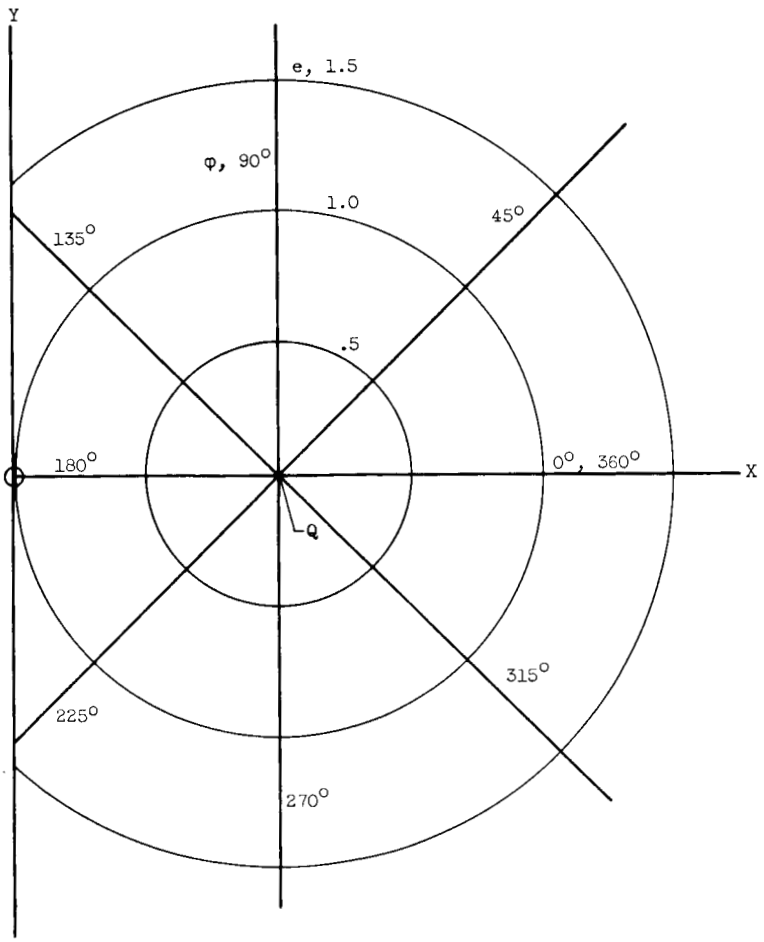

Figure 3. - Polar coordinate system formed by trajectory variables e and φ on X-Y plane of graphical method.

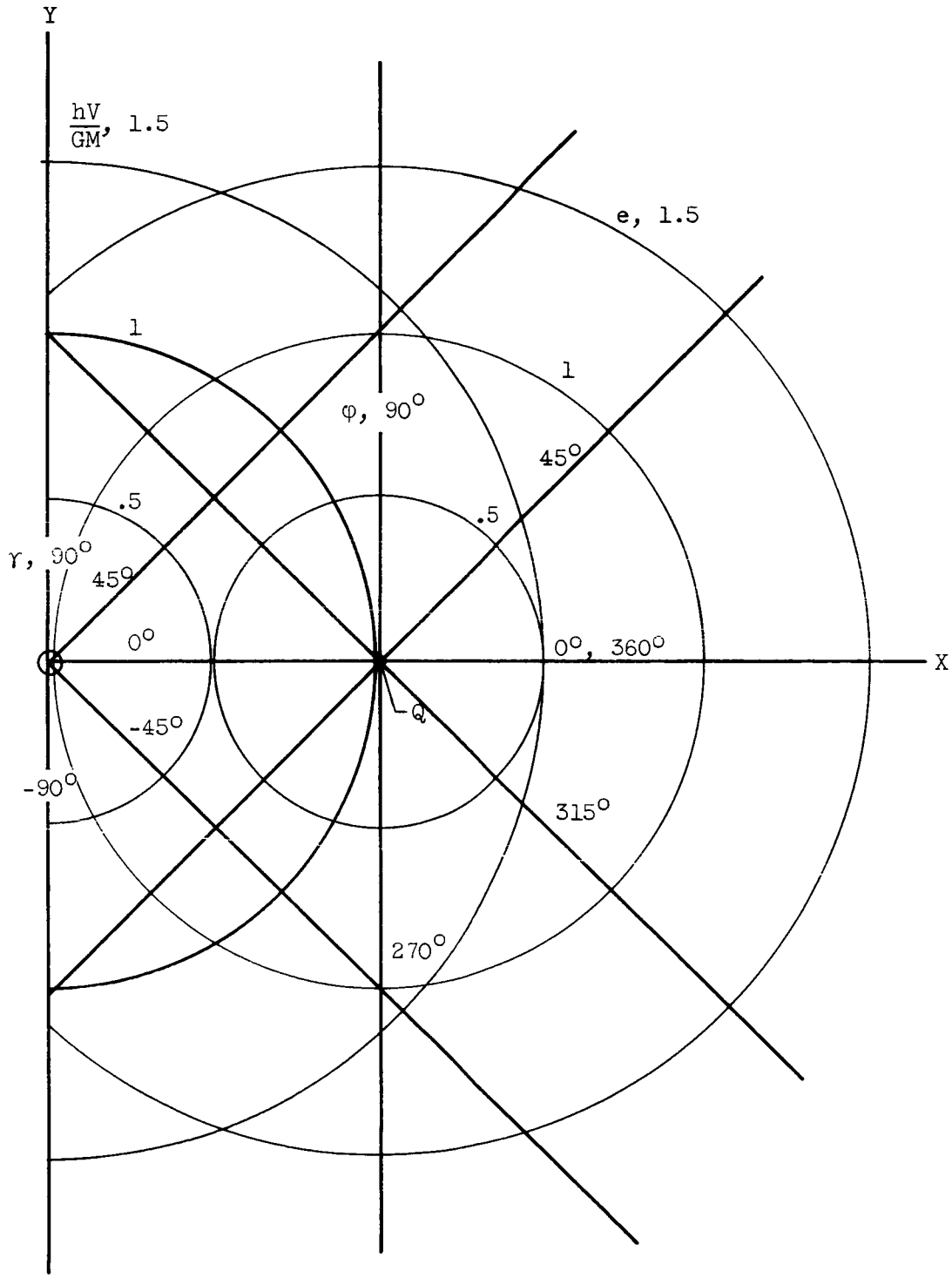

Figure 4. - Two polar coordinates systems formed by trajectory variables e, φ and hV/GM, γ superposed on X-Y plane of graphical method.

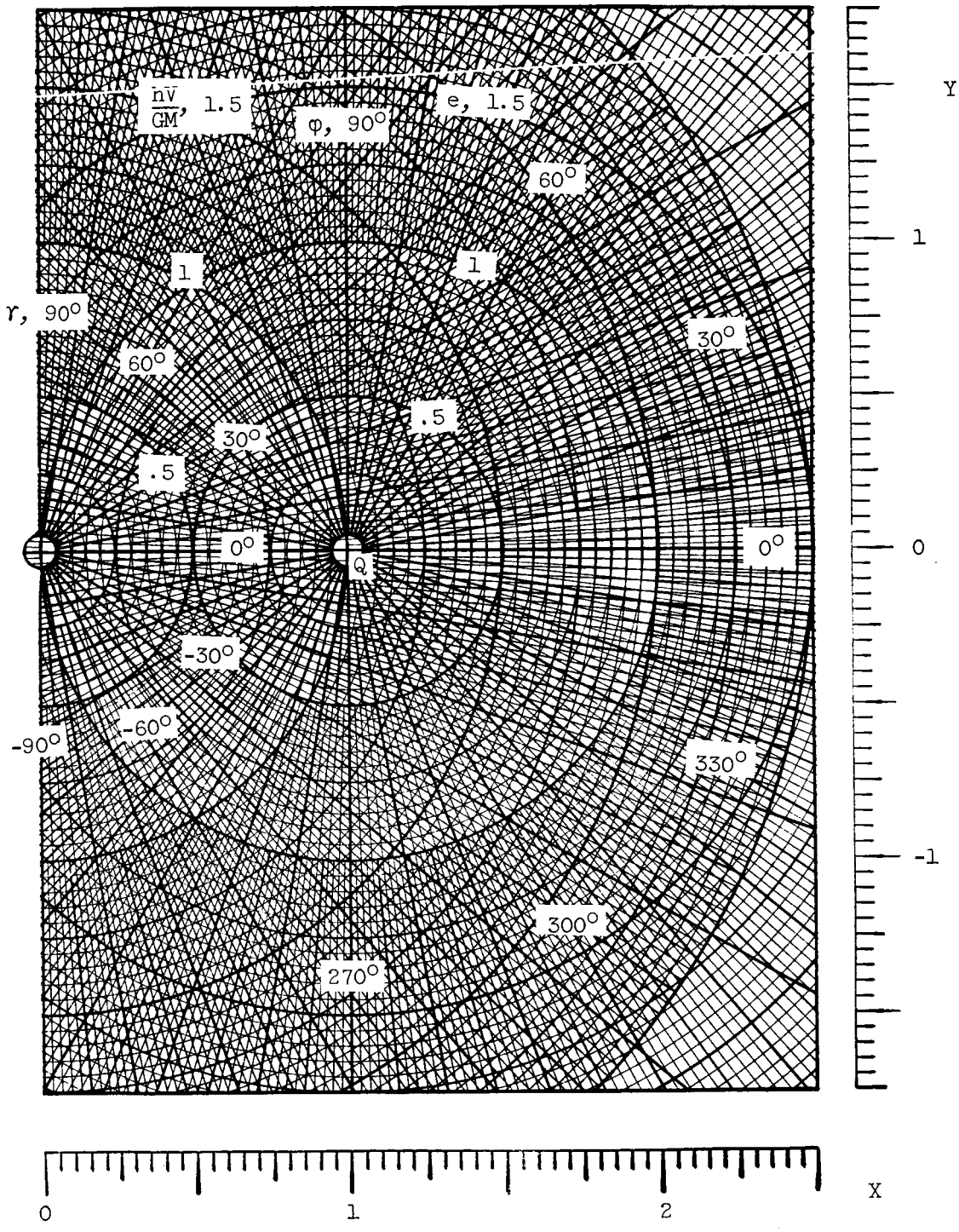

Figure 5. - Detailed grid lines for trajectory variables in X-Y map of graphical method.

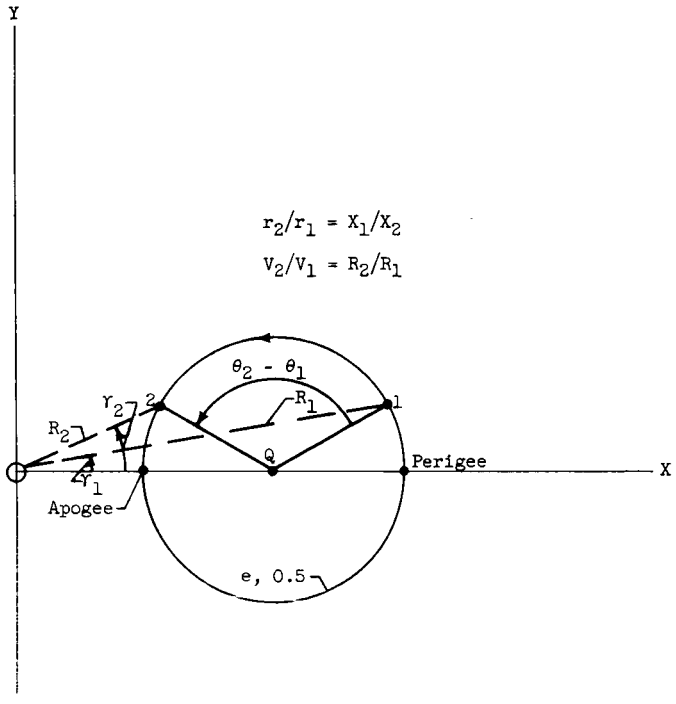

Figure 6. - Example of coasting trajectory.

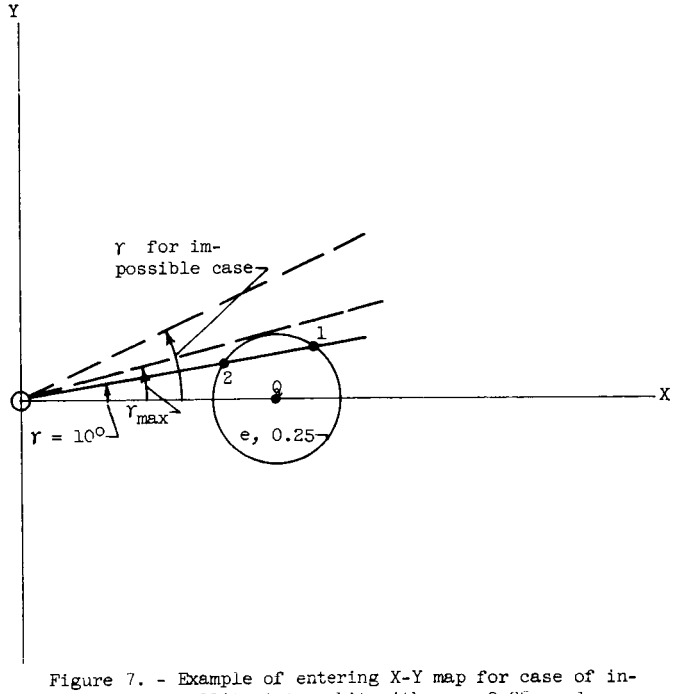

Figure 7. - Example of entering X-Y map for case of injecting satellite into orbit with e = 0.25 and $\gamma = 10^o$ at burnout; illustrating double-valued solution and also possibility of specifying impossible conditions.

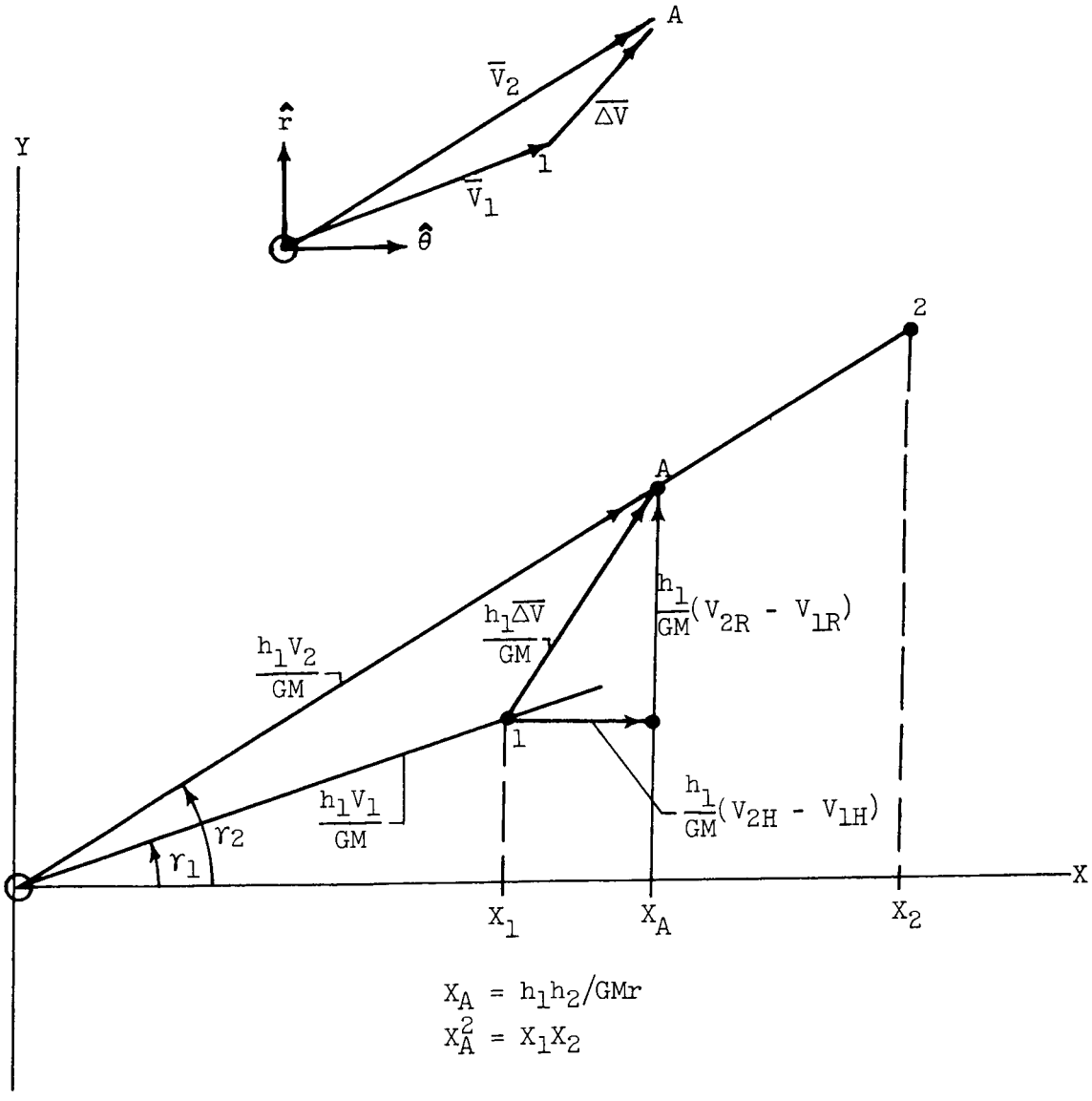

Figure 8. - Construction for impulsive thrust, planar case.

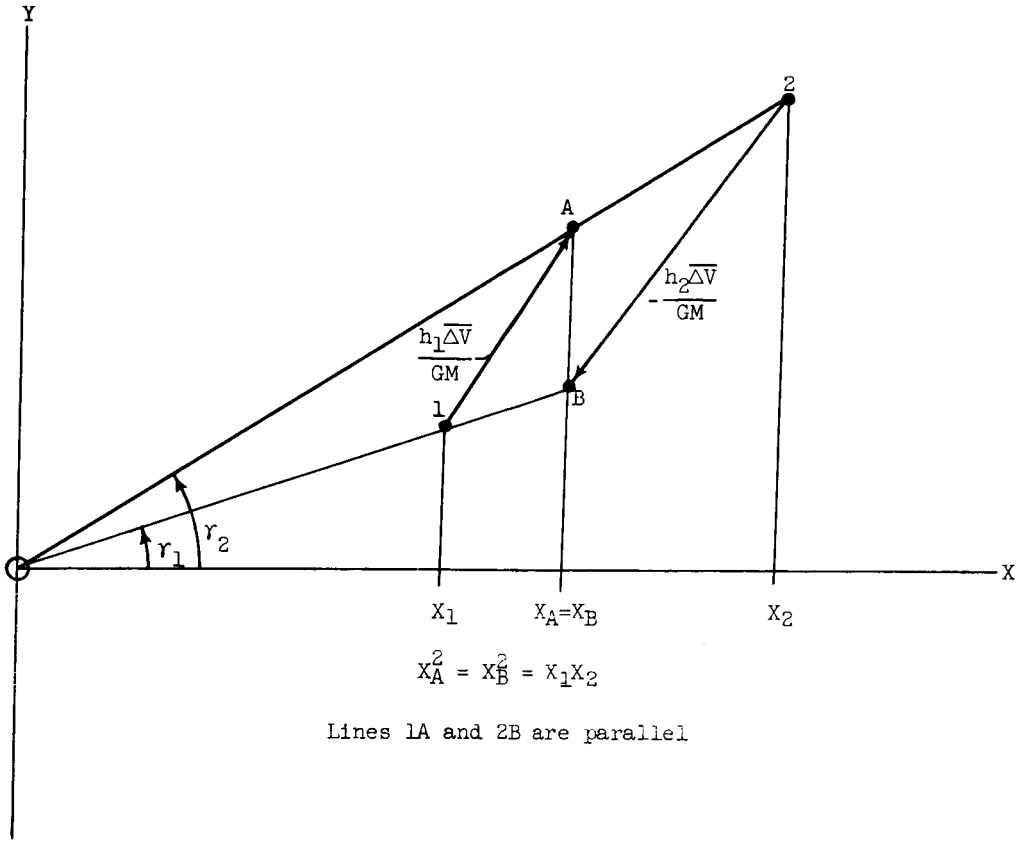

Figure 9. - Relation between forward and backward impulsive thrust.

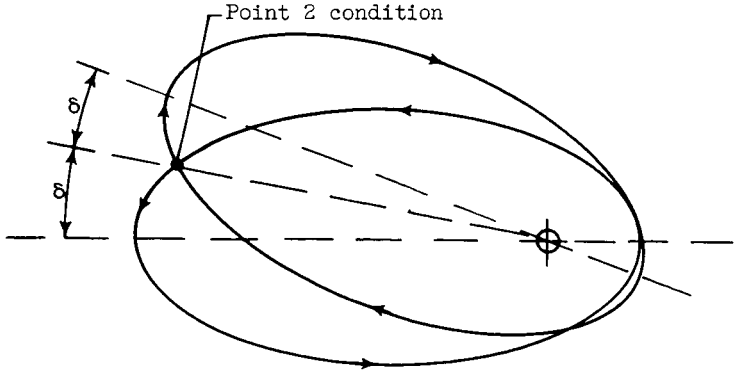

Figure 10. - Trajectories resulting from $\overline{\Delta V}$'s giving mirror image points A on map (figs. 8 and 9), direction reversal.

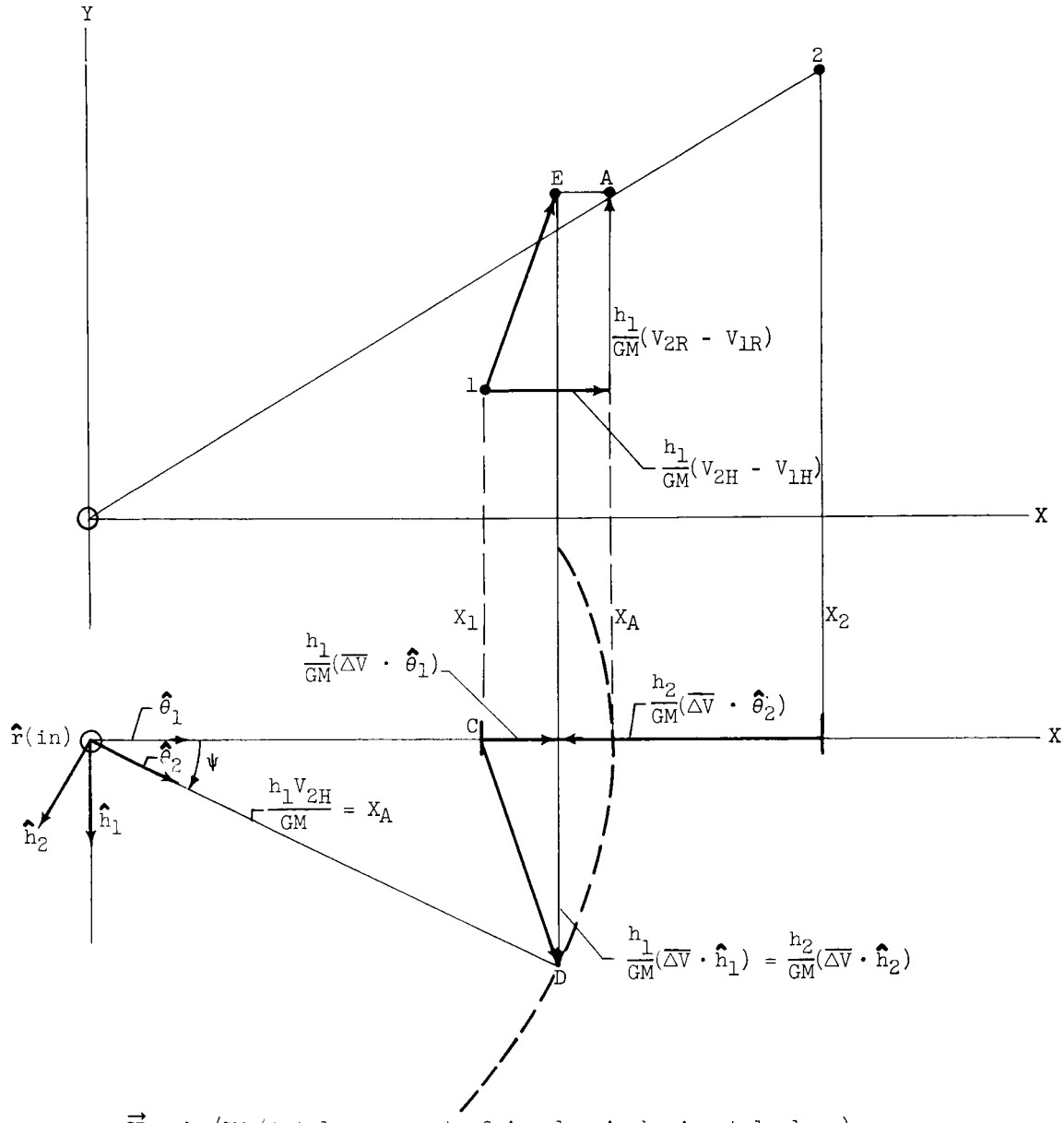

$\overrightarrow{CD} = h_1/GM$ (total component of impulse in horizontal plane)

$\overrightarrow{1E} = h_1/GM$ (total component of impulse in original plane of motion)

$X_A^2 = X_1 X_2$

Figure 11. - Construction for impulsive thrust, nonplanar case.

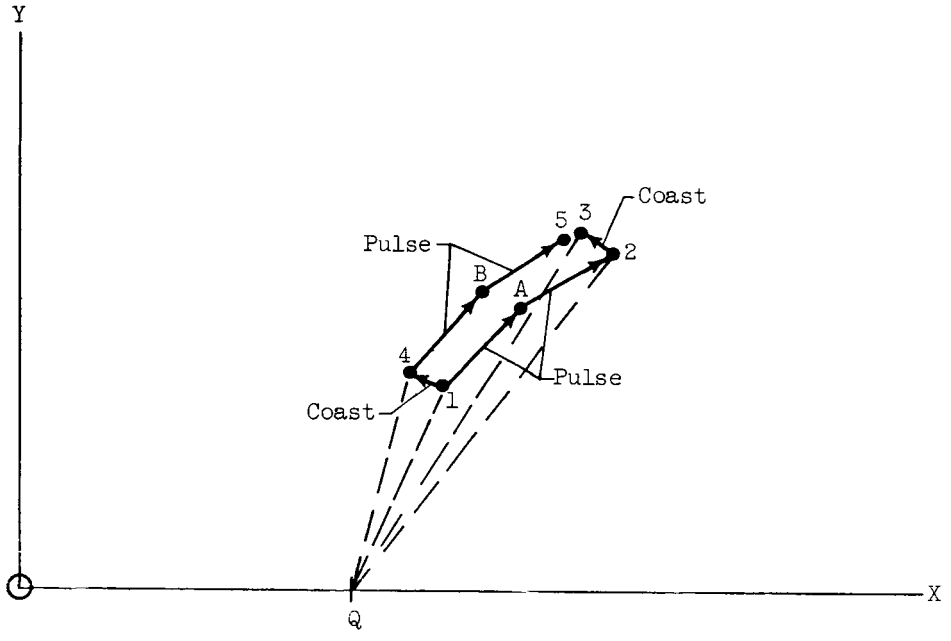

Figure 12. - Construction used in approximation for continuous thrust.

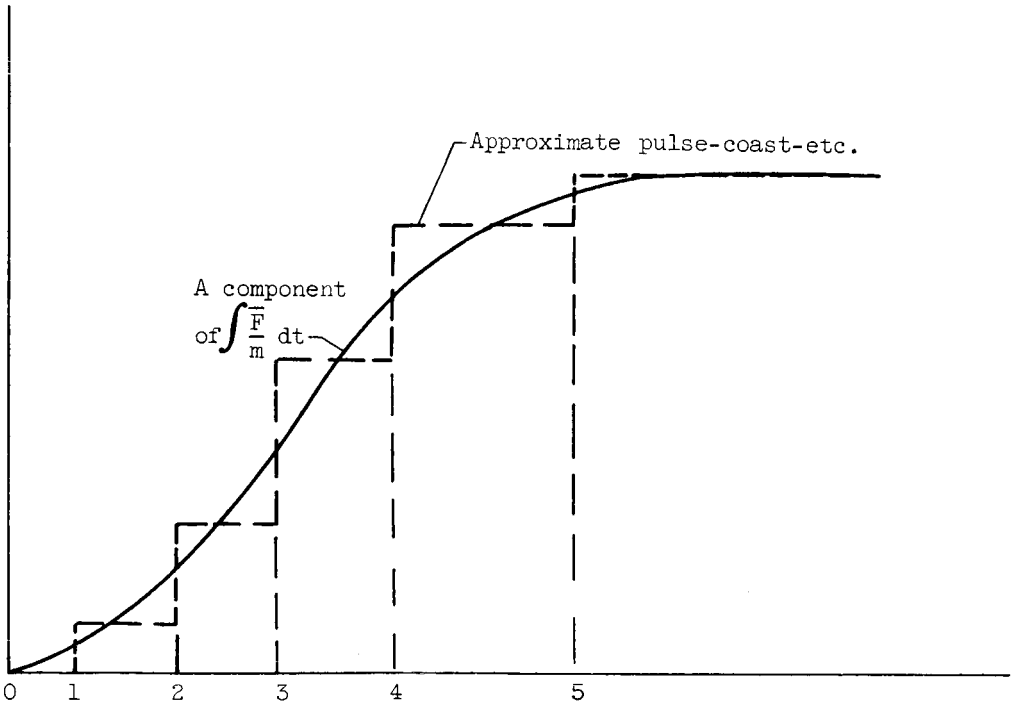

Figure 13. - Typical continuous thrust curve and approximation used in graphical method.

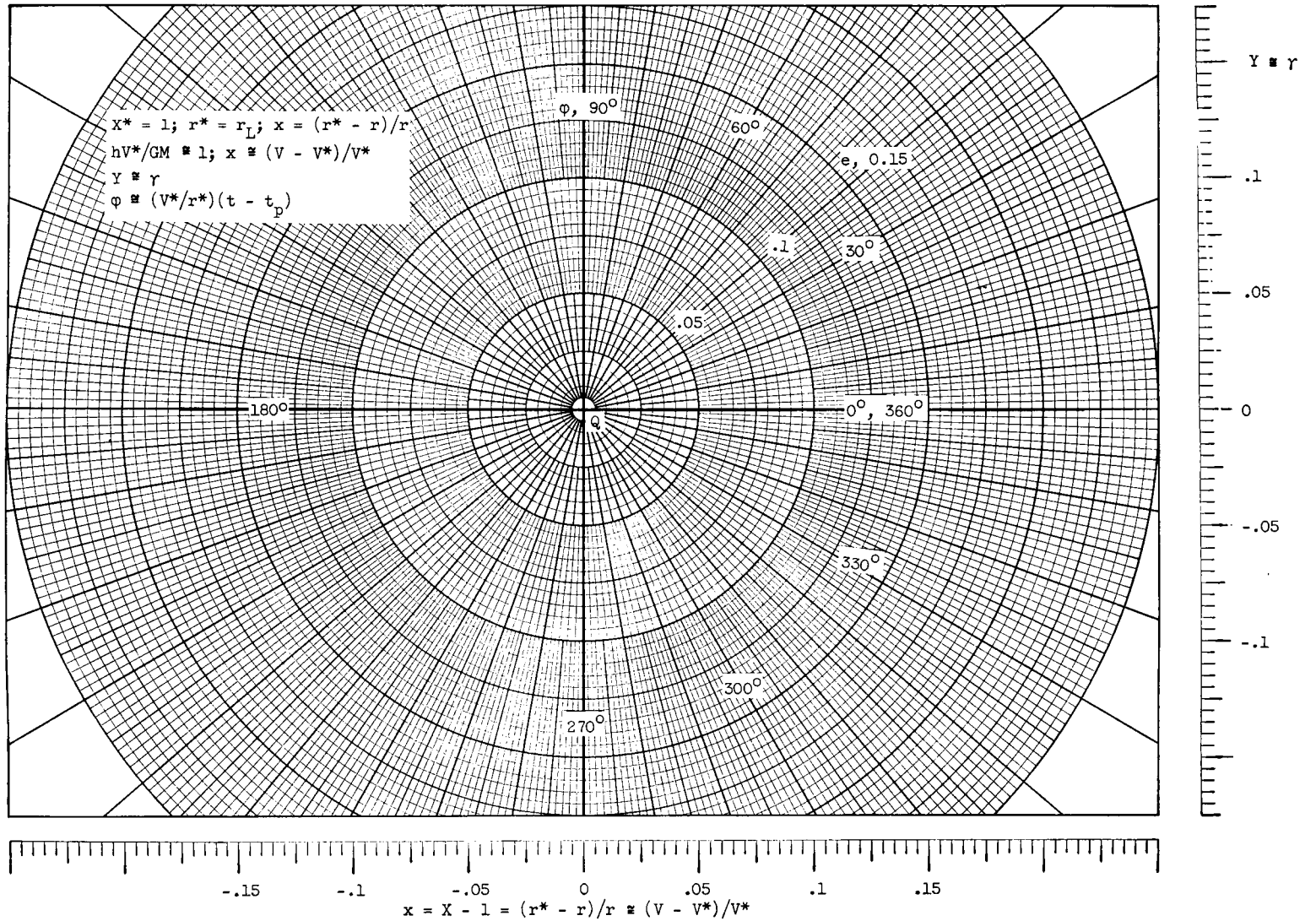

Figure 14. - Approximate map for cases of almost circular orbits, e → 0.

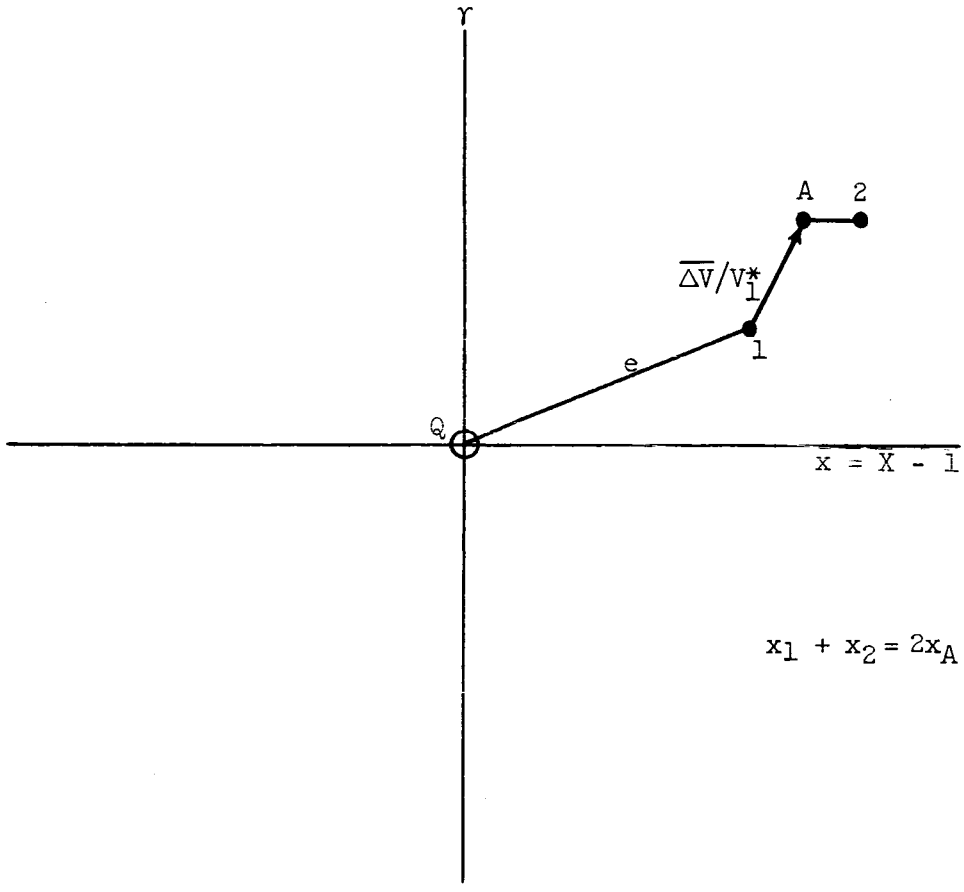

Figure 15. - Construction for impulsive thrust, almost circular orbits, $e \to 0$.

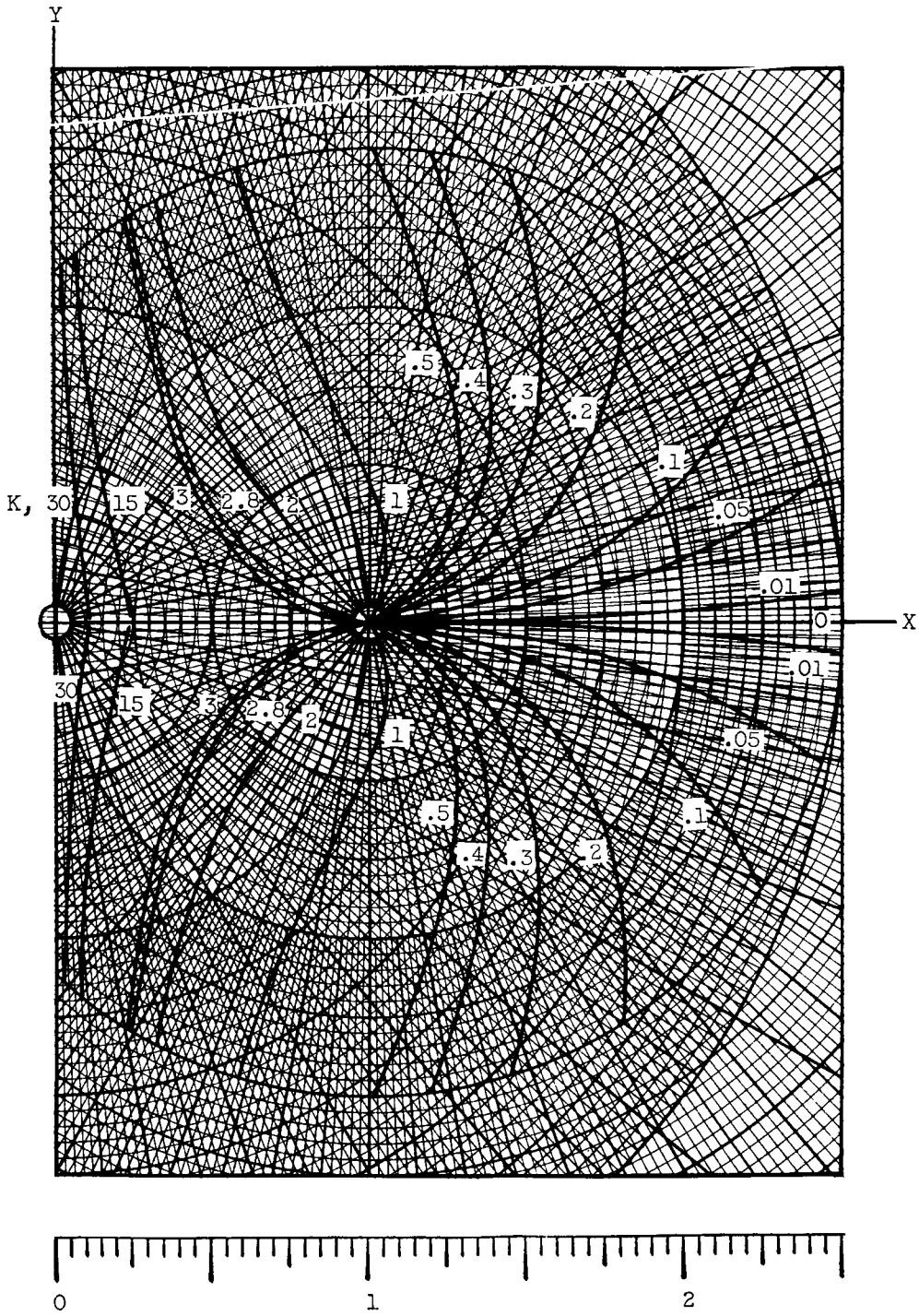

Figure 16. - Time lines on map; lines of constant $K = \frac{G^2M^2}{h^3}(t - t_p)$.

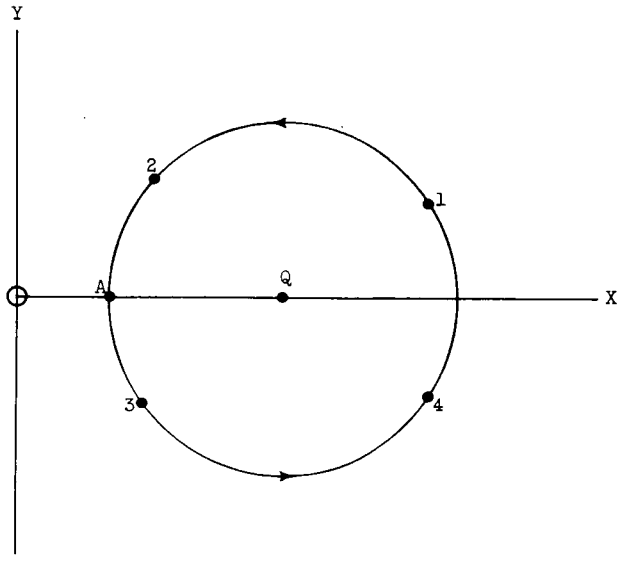

Figure 17. - Four conditions along a coasting path, used to illustrate calculation of elapsed time.

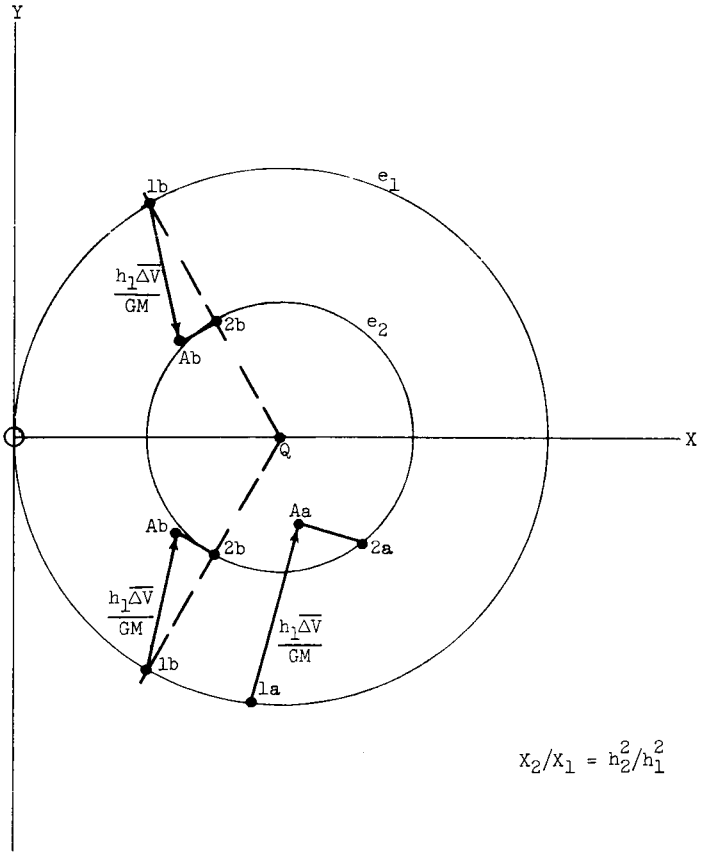

Figure 18. - Examples of transfers to new orbit.

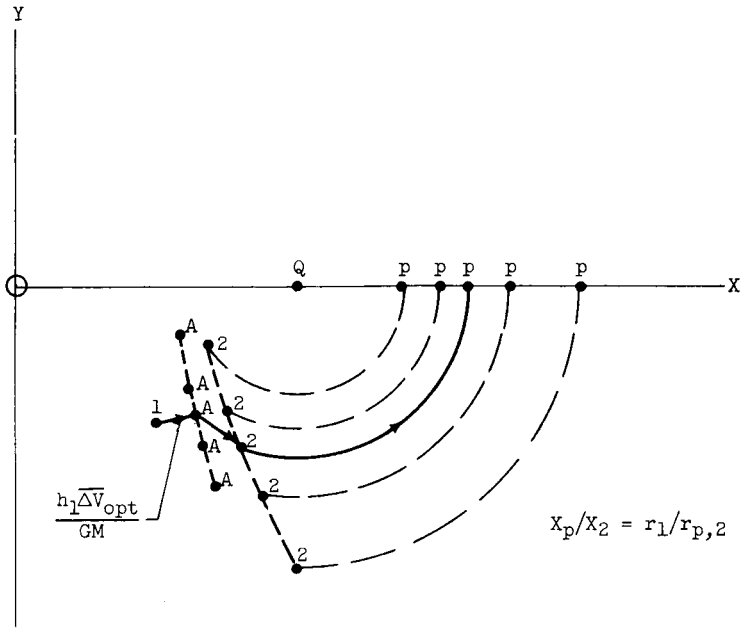

Figure 19. - Example of optimum ΔV, case 1; impulsive thrust applied at definite position along orbit 1 so as to fix perigee of orbit 2 at $r_{p,2}$.

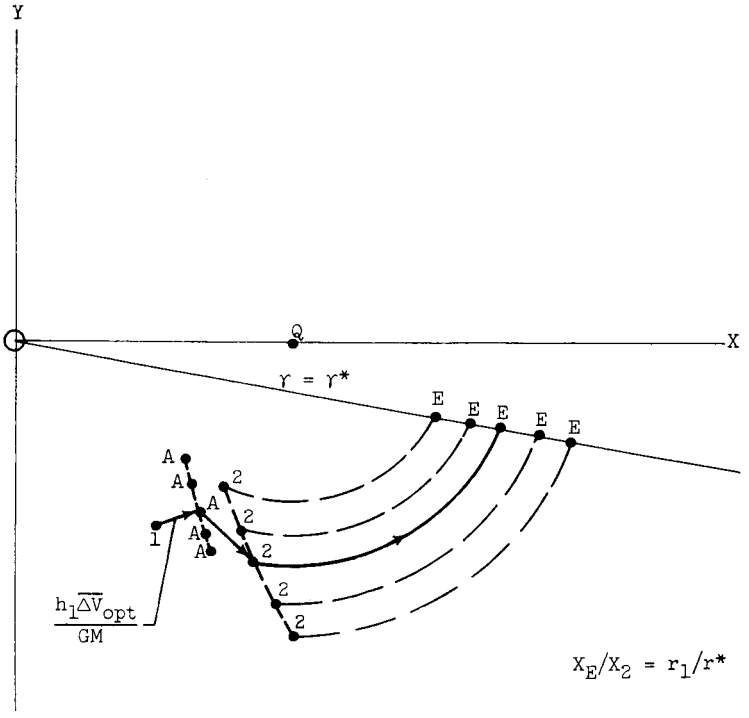

Figure 20. - Example of optimum ΔV, case 2; impulsive thrust applied at definite position along orbit 1 so as to reenter at $\gamma = \gamma^*$ when $r = r^*$.

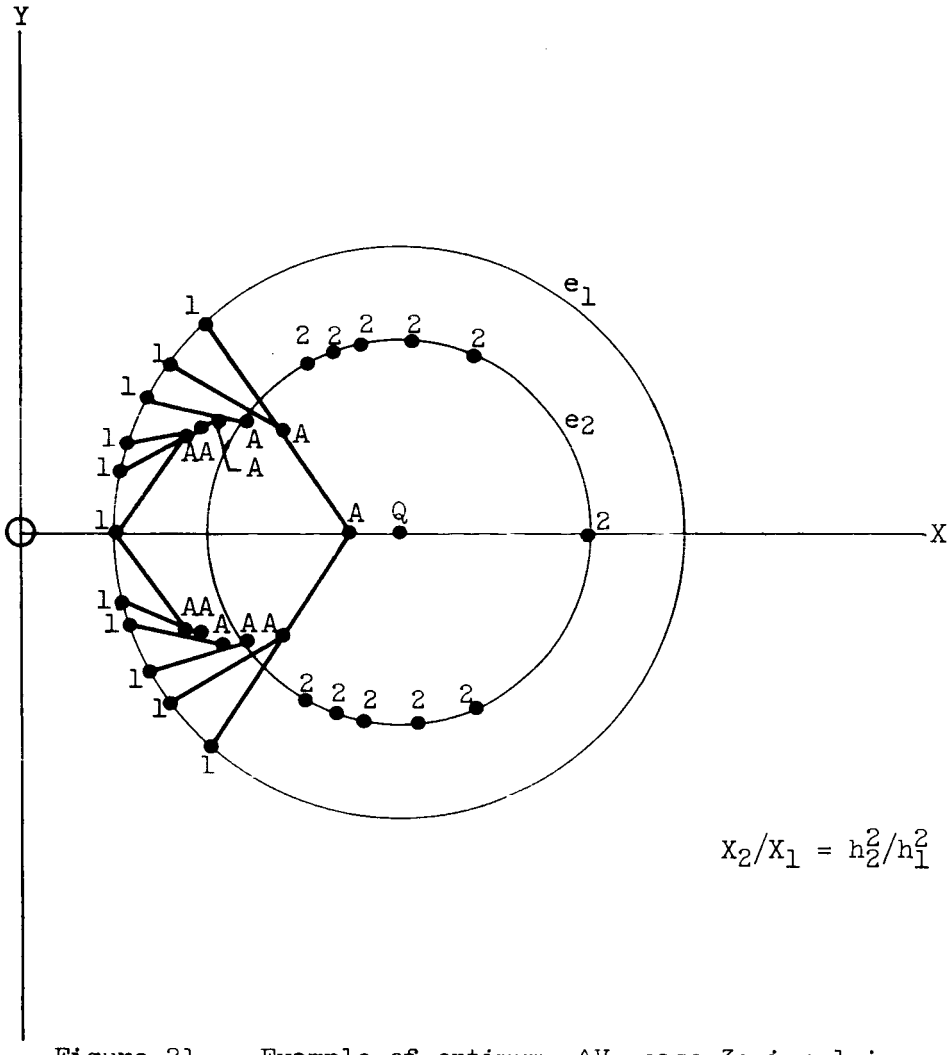

Figure 21. - Example of optimum ΔV, case 3; impulsive thrust applied at any position along orbit 1 so as to change orbital parameters from e_1, h_1 to e_2, h_2.

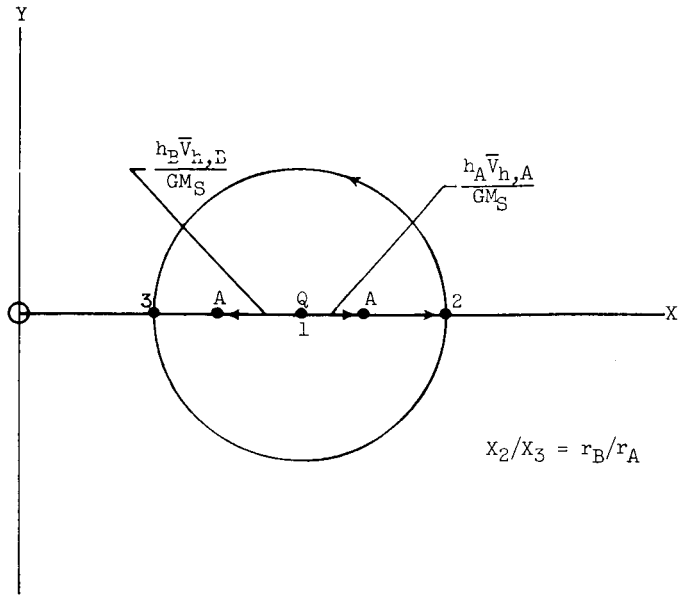

Figure 22. - Example of interplanetary trip; hyperbolic velocities required for minimum-energy transfer orbits.

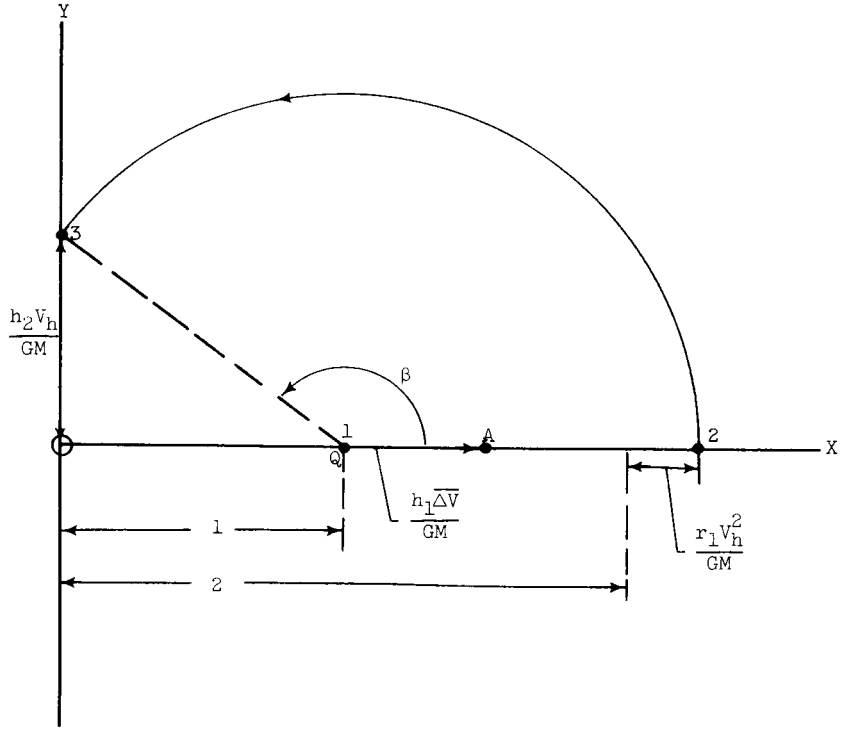

Figure 23. - Example of interplanetary trip; tangential impulsive thrust required for escape with specified hyperbolic velocity, V_h, starting from circular satellite orbit 1.

(1) Angle $(2,Q,1) = \omega_2 - \omega_1$

(2) $X_2/X_1 = h_2^2/h_1^2$

(3) Points O, 1b, and 2b lie on straight line

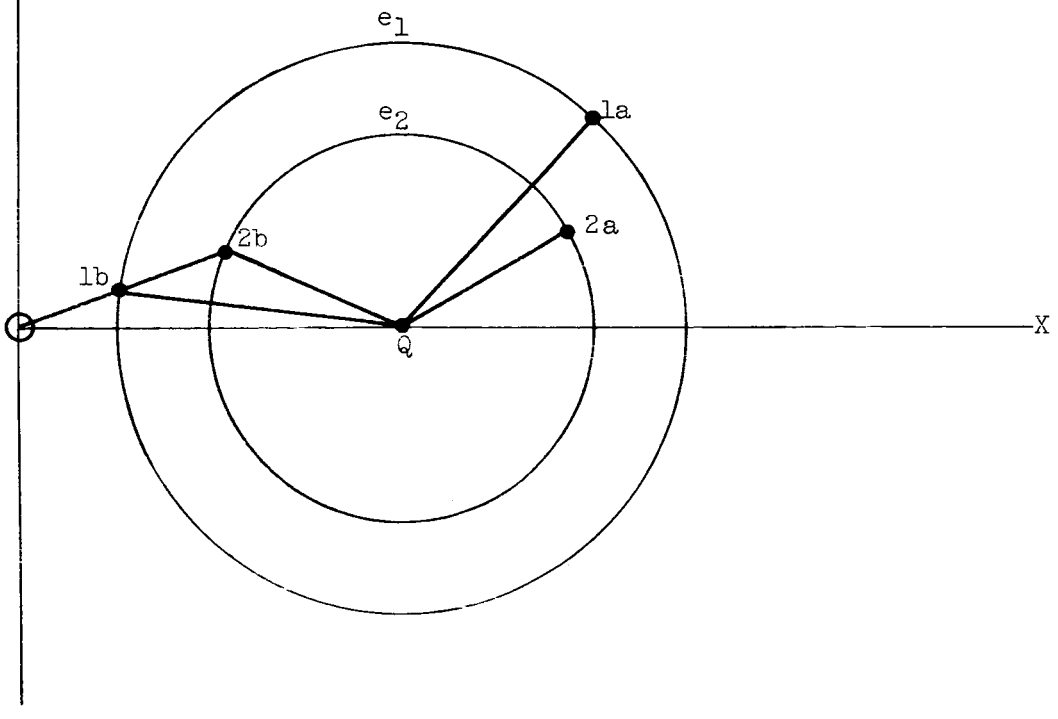

Figure 24. - Illustration of conditions for intersection and tangency of two orbits. Points 1a and 2a are conditions on orbits 1 and 2 at intersection; points 1b and 2b are conditions on orbits 1 and 2 at tangency.

(1) Angle (2a,Q,1) + angle (3,Q,2b) = $\omega_3 - \omega_1$

(2) $X_{2a}X_3/X_1X_{2b} = h_3^2/h_1^2$

(3) Points 0, 1, and 2a lie on straight line

(4) Points 0, 2b, and 3 lie on straight line

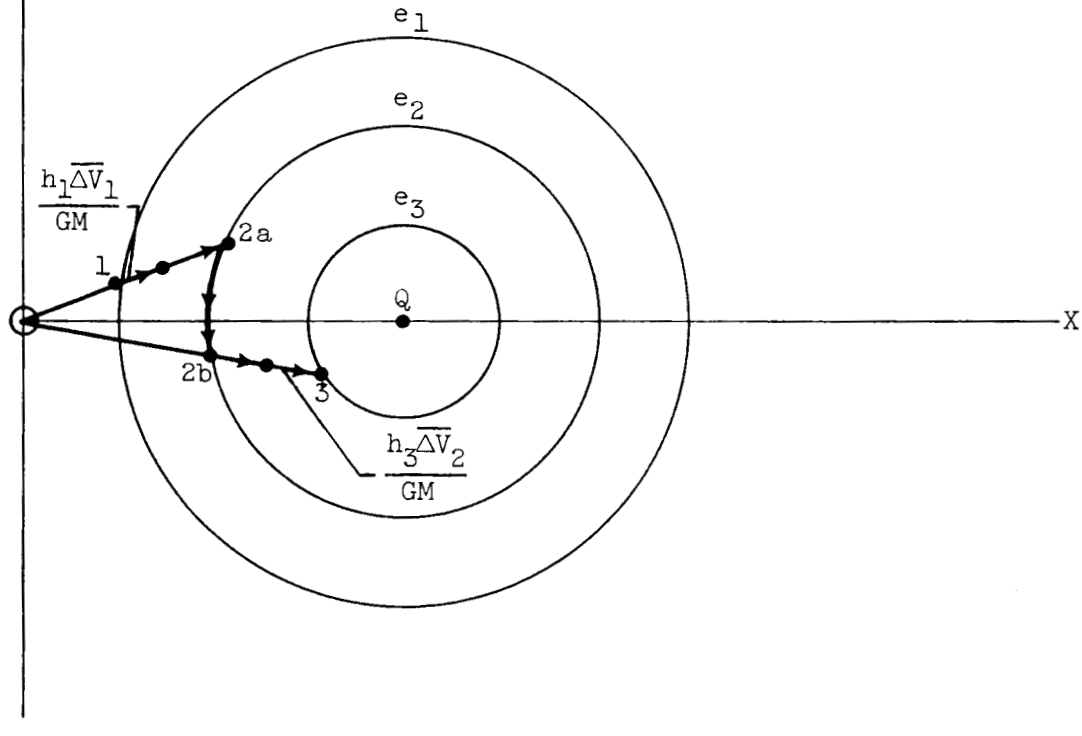

Figure 25. - Example of a rendezvous problem where transfer orbit 2 is tangent to both initial orbit 1 and final orbit 3.

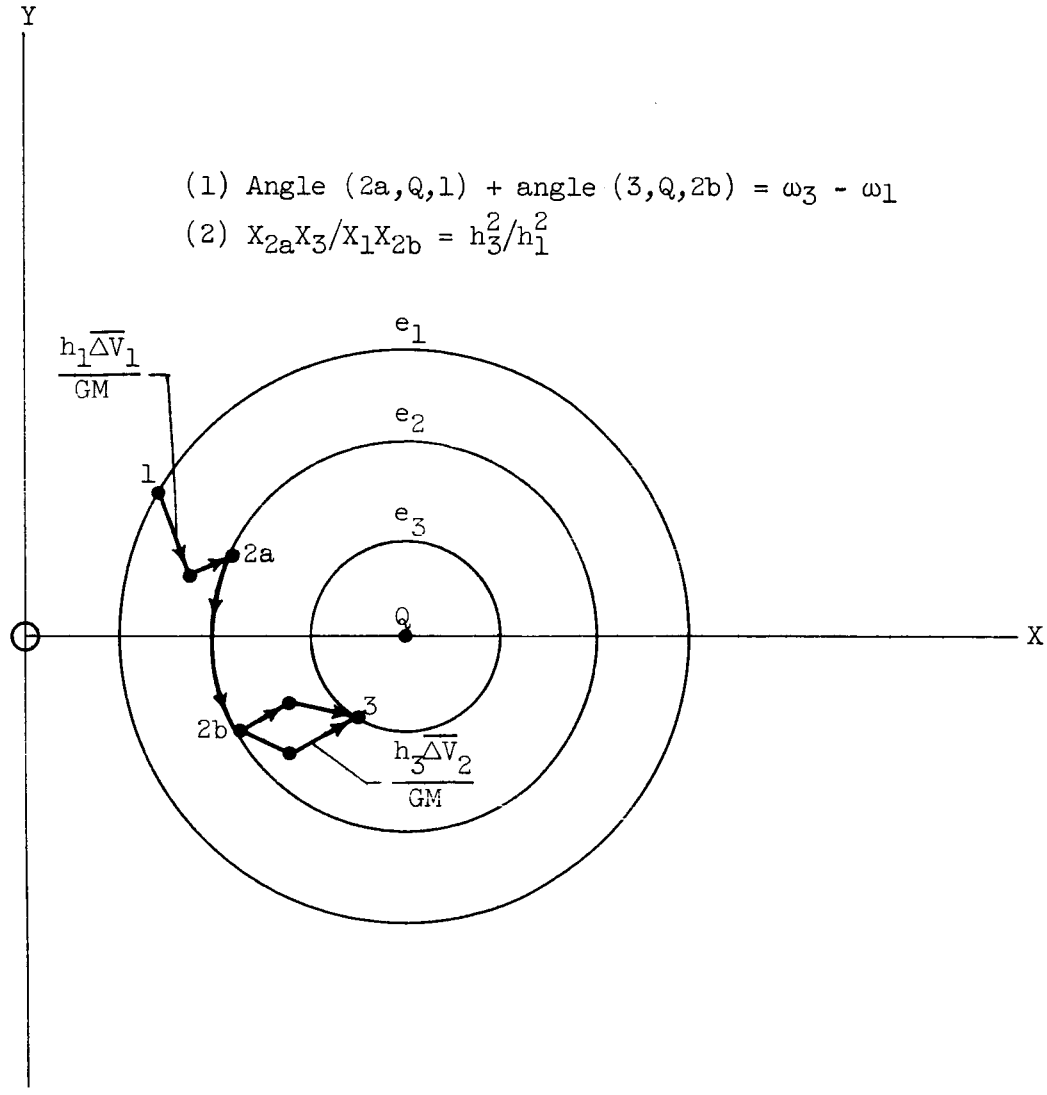

Figure 26. - Example of rendezvous problem where orbital parameters e_1, h_1, ω_1 are changed to e_3, h_3, ω_3 with two impulsive thrusts so that total ΔV is a minimum.

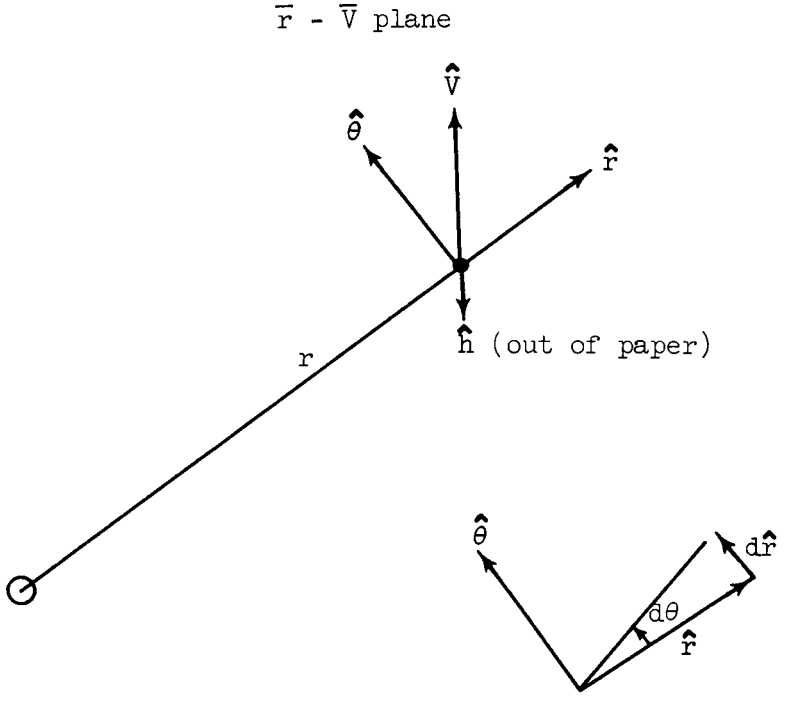

$$\bar{h} = \bar{r} \times \bar{V}$$

$$\hat{\theta} = \hat{h} \times \hat{r}$$

$$\dot{\hat{r}} = \dot{\theta}\hat{\theta}$$

Figure 27. - Instantaneous plane of motion.